ME3 DMT Design Report

E-Bike Frame

Group 1A

Mingquan Cheng
Rohhil Chhabra
Theo Hales
Zhongtian Huang
Rohit Nag

Department of Mechanical Engineering,

Imperial College London

Supervisors:

Dr Liliang Wang
Xi Luan

Page Count: 67
February 26, 2021

Executive Summary

DMT Group 1A was tasked with designing and manufacturing a frame for an electric bike. The purpose of this project was to provide a robust, functional bike frame within budget, which would deliver a smooth ride to the user whilst also housing the necessary systems to drive the bicycle's pedal-assist functionality. This document details the iterations of designing, and assessing the design of, the e-bike frame to be produced by the group, and the processes which enabled its refinement during this time.

This project aims to demonstrate the utility of e-bikes in place of a traditional bicycle, as the pedal-assisted nature of the bike means greater range is easier to achieve for casual riders, and commutes or longer journeys are less arduous. The report details the project objectives, and how these were converted into a design specification. It then follows the design process through the selection of materials and stress calculations, via multiple design iterations to better accommodate the requirements of the other subassemblies.

The results are promising. As indicated by Finite Element Analysis and MATLAB calculations, the frame will function comfortably under normal riding loads, with very low stresses throughout the majority of the structure. Despite additional funding being needed due to the one-off nature of the project, and the potential presence of stress raisers indicated by the Finite Element Analysis, the testing plans aim to scrutinise the areas which are predicted to experience the highest stresses and provide insight into their response to constant and varying stresses.
The results of this design process demonstrate that such a design is possible to manufacture, albeit for just over twice the original budget amount. and this is one consideration that will be taken into the redesign, since the experience of accommodating for the subassemblies and of manufacturing a frame for a low cost will aid the group in refining the budget where possible.

Table of Contents

Executive Summary ii
Nomenclature and Abbreviations v
1 Introduction and Background 1
1.1 Types of Bicycles and E-Bikes. 2
1.1.1 Types of E-Bike assists classes. 2
1.1.2 Types of E-Bike motors and frame positioning. 2
1.2 E-Bike regulations in the UK. 3
1.3 Report structure. 4
2 Project Overview 4
2.1 Brief. 4
2.2 Expected outcomes of the sub-assembly and how this relates to the larger project. 4
2.3 Sub-assembly PDS (working version, at time of writing). 4
3 Description of the design process 8
3.1 Problem analysis. 8
3.2 Primary research. 9
3.3 Early design and intergroup responsibilities 9
3.3.1 Concept Sketches and CAD 10
3.3.2 Intergroup assembly master layout 11
3.4 Material selection. 12
3.4.1 Material selection criterion. 12
3.4.2 Manufacturing considerations. ..... **Error! Bookmark not defined.**
3.4.3 Deriving performance Index 1. 14
3.4.4 Deriving performance Index 2. 16
3.5 Calculation of stresses along tubes. 19
3.6 Frame Redesign Phase 1 22
3.7 Rear Dropouts Design and Disc Brake Specifications 23
3.8 Frame Redesign Phase 2 24
3.8.1 Three part Sliding Dropouts Design 24
3.8.2 Wheel attachment method 24
3.8.3 Considering Rider Anthropometrics 25
3.8.4 Frame Tubing 26
3.8.5 Proposed Mounting Solutions 26

3.9 Design of first iteration for manufacture. 27
3.10 Manufacturing overview 28
3.11 Design for manufacture 28
3.12 Simulation 29
3.12.1 Simulation analyses 29
3.12.2 Initial analysis. 29
3.12.3 Interim analysis; post-redesign. FEA iteration 1. 32
3.12.4 Final analysis 33
3.13 Manufacture methods chosen 39
3.14 Alternative methods considered 39
3.15 How the Manufacturing Readiness Review influenced plans 39
4 Design verification plan 40
4.1 Testing Methods Iteration 1 40
4.1.1 Testing Resources Considerations 40
4.2 Testing Methods Iteration 2 40
4.2.1 Testing Decision Matrix 41
4.3 Dummy Component Testing 42
4.3.1 Selecting Test Components 42
4.3.2 Testing Procedure and Performance Requirements 43
4.3.3 Testing Resources Considerations 47
5 Discussion 48
5.1 Assessment of design objectives. 48
5.2 Budget 50
6 Conclusions 53
7 References 54
8 Appendices 57
8.1 Initial hand calculation of forces along tubes 57
8.2 Example calculation for buckling check 58
8.3 MATLAB Code for FEA. 58
8.4 Shimano Flat Mount Disc Brake Standard 58

Nomenclature and Abbreviations

Symbols	Definition	Unit
A	Cross sectional area of component	m^2
d	The angle frame tube made with horizontal axis	°
E	Young's modulus	N/m^2
F	Force or load	N
F	Force matrix	N
g	Acceleration due to gravity	m/s^2
I	Second moment of area	m^4
k	Stiffness matrix	N/m
L	Length of component	m
P_L	Load needed to buckle	N
u	Displacement matrix	m
W	Weight	N
σ	Stress within a component	N/m^2
CAE	Computer Aided Engineering	-
CNC	Computerized Numerical Control	-
FEA	Finite Element Analysis	-
VAT	Value Added Tax	-

Figure 1: General Terminology for Frame Components.

1 Introduction and Background

Current modes of transportation face a dilemma for the need to travel faster and further while also minimizing the impact on the environment. Electric bicycles have emerged to be one of the solutions to this problem. In their simplest form, e-bikes are regular bicycles driven by electric motors, a concept first patented in 1895 (Ebike Portal, 2015). However, it was not until the start of the 21st century, that electric bikes were commercialised and made available to consumers (Nilesh Bothra, 2019). Continued investment and technological developments such as lithium-ion batteries and smaller motors have propelled the public interest in electrified bicycles, an industry valued at 14.8 billion dollars in 2019 (Paul Lee, Mark Casey & Craig Wigginton, 2020). Despite global sales growing by 23% in 2019 (Holger Haubold, 2020), the adoption of e-bikes has been largely concentrated in areas of pre-existing bicycle demand. In the Netherlands, approximately 45% of all bikes sold in 2018 were e-bikes (Carlton Reid, 2019) compared to only 1.7% in the UK for the same year (Halfords, n.d.). It is evident that there are disparities in motivation for customers and is therefore critical to understand both the driving and restraining factors for e-bike adoption before designing one. In one European focused survey conducted by Shimano in 2019, it was found that a significant portion found e-bikes to be too expensive to consider buying in the future. On the other hand, leisure and commute were found to be the leading driving factors. The results are summarised in Table 1.

Table 1. Summarized data for the barriers and reasons to buy an e-bike among those interested/neutral to use or buy in the future. (https://shimano-steps.com/e-bikes/europe/en/state-of-the-nation-report)

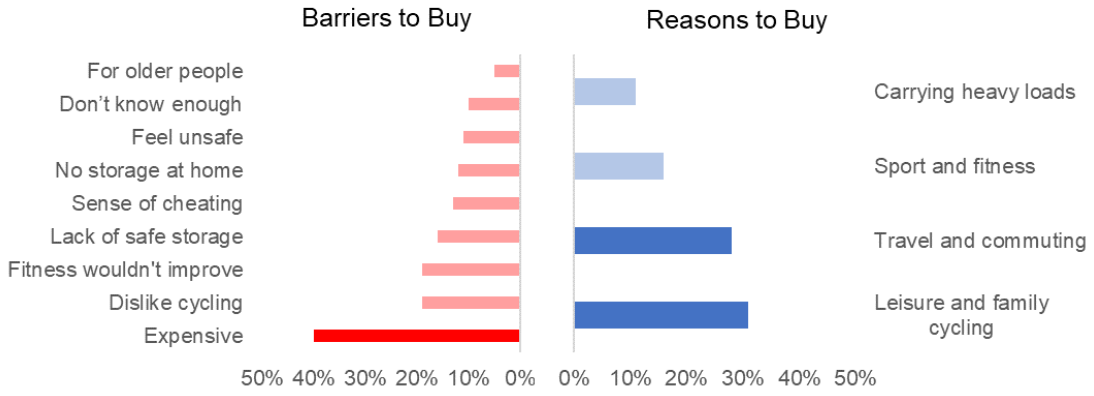

1.1 Types of Bicycles and E-Bikes.

Traditional bikes are categorized based on their intended operating terrain or activity. Most bicycles can be placed under one of the main categories: road, mountain, cyclocross, track, hybrid, and city. Differences between categories are defined by changes in the frame geometry, frame stiffness, wheel size, rider position, suspension type, and tyre width. Fine-tuning these characteristics influences the bicycle handleability, terrain adaptability and rider comfort.
E-Bikes are categorized similarly to their mechanical counterparts, however, are more commonly manufactured as one of these four main forms: comfort, commuter, road or off-road. Due to the addition of a motor and battery, e-bikes are also classified by the type of assist. (Claudia Wasko, n.d.) and the type of motor itself. Depending on the motor and assist type, manufacturers must carefully alter the frame and other components to maintain the ride type of the required form.

1.1.1 Types of E-Bike assists classes.

Class 1: Pedal-Assist:
Limited to a top speed of 25 kph, class-1 e-bikes feature no throttle to control the motor. Instead, the motor only provides power during pedal strokes from the rider.
Class 2: Throttle Control:
Limited to a top speed of 32 kph, these e-bikes operate similarly to motorcycles or mopeds where the motor output is directly controlled by the user using a throttle on the handlebar. The throttle could be by an analogue lever or an actuator switch.
Class 3: High Speed Pedal-Assist:
In principle, class 3 e-bikes are identical to class-1 in terms of operation but have a higher speed limit of 45 kph.

1.1.2 Types of E-Bike motors and frame positioning.

There are two types of motors used in e-bikes and three conventional mounting locations used commercially (GREATEBIKE, n.d.).
Hub Motors:
The most common form are hub motors which drive the wheel directly. As seen in **Error! Reference source not found.**a, by mounting on the front or rear wheel axle, valuable space is saved on the main frame. Due to its form factor, regular bicycles can easily be converted into e-bikes working on throttle functionality. However, by attaching to the wheel directly, the (often heavy) hub motors can act as large un-sprung weights on the wheel and can lead to fractures in

the dropouts (Eric Hicks, 2012). Furthermore, regular user repairs of the bicycle such as changing flat tyres or re-attaching a dropped chain can become difficult tasks.

Mid-Drive:

Mid-drive motors mount on the bottom bracket and drive the pedal cranks as shown in Figure 2b. Generally featured on higher performance bikes, mid-drive motors solve few of the issues found on hub-motor driven bikes. Firstly, by driving the cranks instead of a wheel, pedal assisted features can be incorporated. Additionally, the central mounting location is closer to the centre of gravity providing greater directional stability.

However, the positioning of the motor means that mid-drive e-bike frames need to be carefully designed around the motor placement. This is because this region is the joining point of three load-bearing frame components: the downtube, seat tube and chain stay. The complexity of the design has led to many specialist manufacturers such as Bosch to solely focus on mid-drive solutions including mounting brackets (Claudia Wasko, n.d.).

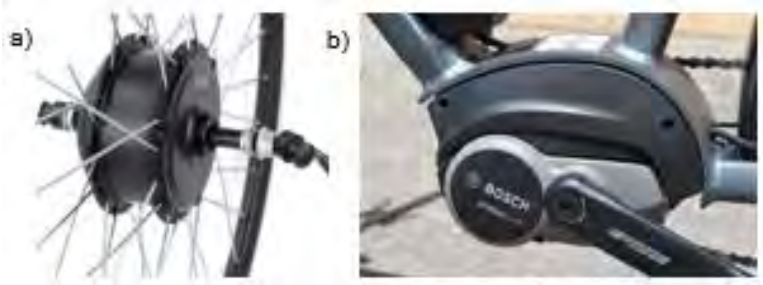

Figure 2: a) A commercially available hub motor mounted on the rear wheel (Direct Voltage n.d.) and b) A mid drive motor solution by Bosch demonstrating the additional complexity of the frame design (Mikey G, 2019).

1.2 E-Bike regulations in the UK.

It is crucial to understand the safety implications of electrifying a bicycle. For example, class-2 e-bikes can pose the danger of unknowingly applying too much throttle from a high gear when starting. More worrying, electrical stalls during operation at high speeds can cause major accidents. In the UK, e-bikes must meet a certain range of requirements (GOV.uk, n.d.). E-bikes are restricted to only class-1 equivalent bikes also known as ‘electrically assisted pedal cycles’ (EAPCs). Regarding the performance, bikes must be limited to a maximum output power of 250 watts and maximum speed of 24.9 kph.

1.3 Report structure.

Section 2 explains the project objectives which are quantified in the product design specification section. Section 3 follows a semi-chronological order and conveys the entirety of the design process involved. Sections 3.4 and 3.5 explain how materials analysis and analytic calculations were used as tools for developing the initial concepts shown in section 3.3. After further iterations are explained, the final design for the first iteration of manufacturing is showcased in section, followed by the manufacturability aspect of the design. The design process section is concluded with FEAA simulations and design validations. Extensive testing considerations and planned verification methods are discussed in the following section. This includes the components being tested and the relevant testing equipment. The success of the overall design based on the meeting the PDS objectives and budgeting constraints are discussed in section 5 before the conclusion.

2 Project Overview

2.1 Brief.

The initial brief for the overall project encapsulated designing and manufacturing an e-bike from the ground-up. A few important feature requirements were proposed by the design supervisors: It meets the legal specifications for e-bikes in the UK, has no hub motors, is foldable, fits into a suitcase and the entire assembly should be less than 30 kg.
Expected outcomes of the sub-assembly and how this relates to the larger project.
The expected outcomes of this subassembly were to produce a robust, functional bike frame strong enough support the rider during operation, whilst remaining light. The relevant subassemblies needed to be accommodated for this sub-assembly, and indeed the project as specified, to be a success. (The steering assembly must fit into the head tube, for example, and the battery and motor assemblies must be incorporated into the frame, as per the brief).

2.2 Sub-assembly PDS (working version, at time of writing).

Element	Criteria	Verification	Date Modified
User Experience			
Needs	To accommodate for a comfortable ride	Market Research on what is preferred and required.	05/11/2020

	position. Battery module must be integrated into frame.		
Market	Type of bike and specific features must fit city cycling requirements.	Research and compare to current urban, hybrid and road bikes.	05/11/2020
Physical Properties			
Size	54cm frame designed for a rider of height (169-176cm). Reach of approx. 380mm and handlebar height of approx. 830mm.	Research average human dimensions and corresponding frame measurements.	05/11/2020
Weight	Overall weight range: 15-30kg Frame weight range: 8-14kg	Calculate material weight using overall dimensions before manufacturing. Confirm weight by weighing manufactured frame.	05/11/2020
Wheels	700cc (622mm) Quick release mechanism.	Will be purchasing wheels. Detailed stress analysis will be performed to verify frame compatibility.	05/11/2020
Material	Must be able to withstand impact stress tests according to British standards. Must meet frame weight range. Corrosive and weather resistant.	Material Selection through CES Material Package.	05/11/2020

Cables and Wiring	Must accommodate for connections to motor and battery. Internal wiring reviewed; not employed on first iteration.	Review with drivetrain, battery, and motor team.	16/02/2021
Shape	Avoid having sharp edges and corners.	FEA analysis and design review.	05/11/2020
Saddle and seat-post	Frame must accommodate for standard 27.2mm seat post.		05/11/2020
Fenders and mudguard.	Mudguard attachments for front were responsibility of steering group. Rear mudguard does not need explicit attachment as it can clamp to the seat post.		16/02/2021
Performance			
Fatigue	Must be able to withstand cyclic forces to simulate riding conditions on the road and pedalling forces.	Testing according to (BS EN 15194:2017) sits outside of the budget of the group and specialized rigs for these tests are costly to produce and obtain. Tests also call for deformation of the frame which serves to weaken the bike; dummy component test methods will be employed. (to avoid damaging the original frame). FEA to be used to predict most vulnerable components.	26/02/2021

		Verification by visual inspection of visible cracks or fractures in the assembly. There should also be no separation of parts at the joints.	
Impact Resistance	Must be able to withstand direct impact forces (horizontal and vertical) in cases of unnatural conditions and collisions.	Visual inspections of deflection and cracking performed under loading. FEA to be used to predict most vulnerable components.	26/02/2021
Bending, deformation and stress.	Frame must be able to support an 80kg rider under static stresses.	Measurement of stresses required to cause complete failure of critical components taken with Instron machine. FEA modelling and stress analysis used to predict most vulnerable components under largest stress.	26/02/2021
Operating Environment	-5°C - 40°C for wide range of cities	Select materials based on these operation temperatures.	26/02/2021
Safety factor	Frame must exhibit a safety factor of 3 under normal riding loads.	FEA modelling.	26/02/2021
Life Span			
Product Life	5 years	To be considered during material selection and calculation	05/11/2020
Service Life	10 years		05/11/2020
Production			
Quantity	10 million.	To cater for the ever-growing need for urban transportation	05/11/2020
Product Cost	4 times of manufacturing cost Market price is around £1000-£10000	Calculation of cost of material when bulk purchase, cost of manufacturing	05/11/2020

Manufacturing Cost	Price of components and material with various manufacturing methods		05/11/2020
Regulatory			
Safety Standards	Compliance to all BSI Standards	Conform to BS EN 15194:2017 where possible	05/11/2020
Environmental Impact	Sustainable materials where possible	Source sustainable materials	05/11/2020
Production Regulation	Compliance to BSI Standards	Reference to BS EN 15194:2017 – testing methods to be assessed comparable to this where possible, but see previous performance section for assessment of validity of testing to this standard.	16/02/2021

3 Description of the design process

Due to the inter-group nature of the project, certain specifications remained fragile throughout. Despite careful inter-group planning certain abrupt changes were inevitable and did occur. As such, a total of five complete redesigns were necessary before all requirements were met. While not all designs are mentioned in detail in this section, key design decisions are explained and presented in a chronological manner to capture the iterative process.

3.1 Problem analysis.

This DMT project aims to design a bike frame as per the requirements in the PDS. The bike frame must fulfil these requirements, including with reference to rider weight and position, mass of the frame, and compatibility with and integration of the other sub-assemblies. It must also be manufactured and tested on time while remaining as close to budget as possible. The element of integration of the sub-assemblies was one of the most significant, since it is integral to the classification of the bike as an e-bike. Besides, FEA analysis needs to be carried out throughout the design journey to validate the structure rigidity of the frame.

3.2 Primary research.

The design journey began by taking inspiration from existing e-bikes on the market. The goal was to understand why certain design decisions were taken by established manufacturers and what these achieved. The areas of specific interest were the battery mount, motor mount and frame geometry. To get a broad understanding, three e-bike frames of different categories, were compared and analysed as shown in Figure 3.

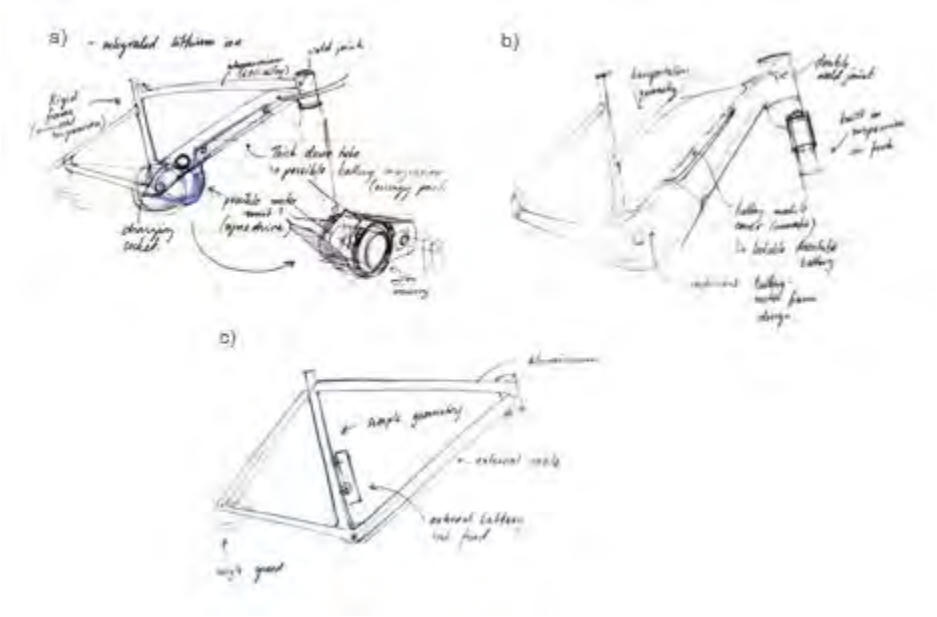

Figure 3: Comparison of design features in a) Giant FastRoad E+Pro, b) Specialized Turbo Vado 3.0, and c) Ampler Curt e-bike.

The analysis was also helpful for gathering geometric frame data for our target consumer, an average UK male. The suggested size from most frame manufacturer websites was found to be 54cm for this target consumer (Evans Cycles, n.d.; Specialized, n.d.).

Having initially decided on making a road-focused bike, a range of data from popular 54cm road e-bikes were noted and averaged. This initial research data would form the basis of following concept sketches and initial master-layout used for the entire inter-group assembly.

3.3 Early design and intergroup responsibilities

While each of the four sub-groups had a general idea of their respective roles, the exact limits of each assembly were clarified during the first few meetings. Initial allocation was solely based on group preferences, however, was later reworked to incorporate potential budgeting imbalances. The map in Figure 4 illustrates the final allocation of roles between the teams.

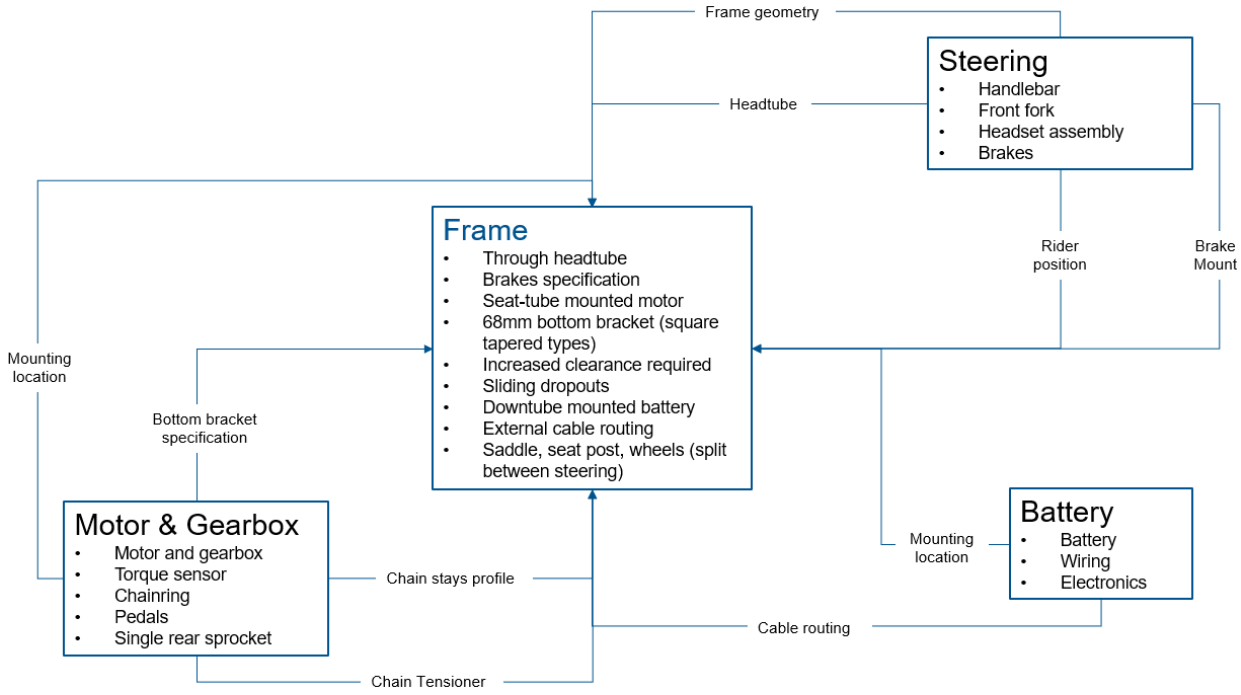

Figure 4: Final intergroup responsibilities allocation.

3.3.1 Concept Sketches and CAD

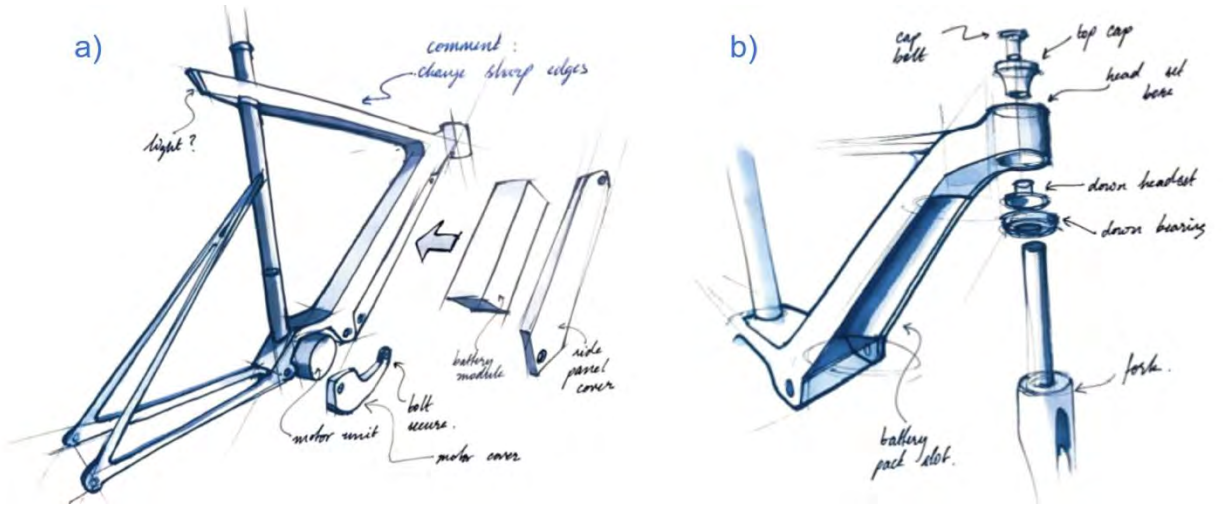

Figure 5: Initial concept sketch showing how the a) battery, motor, and b) steering subassemblies were proposed to fit together.

The initial concept design as shown in Figure 5 was inspired by the primary research conducted as mentioned in Section 3.2. The primary focus of this design was to meet the “all parts shall be integrated into the frame” requirements mentioned in the PDS. This design was translated into CAD and was later developed into the first iteration of the frame design.

Figure 6: First concept CAD model.

As shown in Figure 6, the concept frame featured a battery cut-out in the downtube and a motor bracket integrated into the frame. Horizontal dropouts joining the seat stays and chain stays were designed for easy wheel attachment and chain tensioning.

3.3.2 Intergroup assembly master layout

Apart from defining the boundaries, achieving cohesion between the sub-groups was of upmost importance. Throughout the design process, the design was standardised within the overall project by the frame team. This was done by providing a skeleton layout including all the critical dimensions as shown in Figure 7, to all sub teams. Initially, these dimensions were based on existing bikes as mentioned in Section 3.2, however were later customized based on human anthropometrics (See Section 3.8.3) and digitalised as a CAD sketch. This method was also used to assign allocated geometric limits for other subgroups as agreed upon.

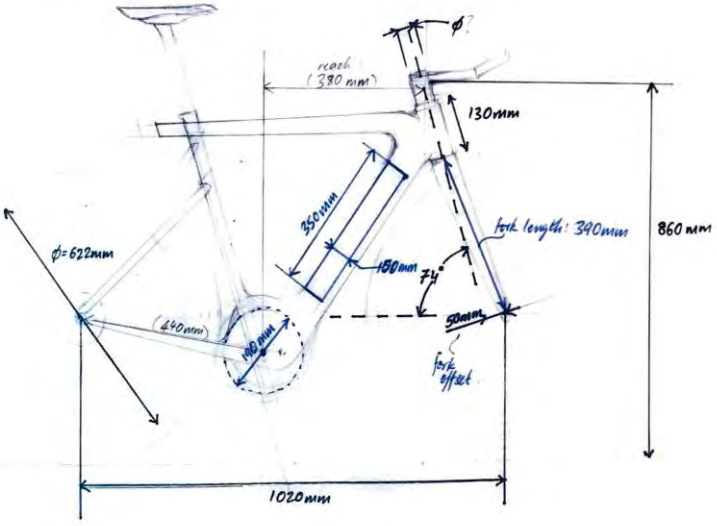

Figure 7: Initial master layout sketch of the frame which was provided to all sub-teams.

3.4 Material selection.

Material analysis was done after the initial concept to understand the manufacturability constraints on the design as well as potential structural limitations. An overarching constraint was to minimise the cost with respect to any given performance metric, to ensure that the greatest value for a given material or component was achieved.

Table 2: Material selection criterion.

Criterion	Justification (Why it matters)
Cost	Given a strict £1,000 budget, it is important that the selected material is affordable and easily available.
Yield Strength	A strong bicycle with high resistance to plastic deformation upon impact is key a factor in durability
Density	Given a weight target for the frame defined in the PDS (8-14kg), material density informs dimension decisions that allow a lighter structure. The weight of the bike is a key factor in determining how transportable it is.
Young's Modulus	The stiffness of the frame is important in determining how efficiently the rider's pedalling transfers onto the road. Hence, a stiffer bike frame is more desirable. Practically however, stiffness is dependent on both Young's Modulus and geometry.
Toughness	It is important for a bike to withstand shocks from uneven terrain; hence it should be able to absorb the shock energy without fracture.
Fatigue Strength	Because electric bicycles are made with the purpose of daily transportation, they have to withstand repeating loading cycles.
Corrosive Resistance	As an outdoor transportation device, it is key that the frame is resistant to rain, mud and UV.
Ductility	In the event of a crash or large impact, the bike should be able to sustain sufficient plastic deformation and provide sufficient warning before failure. Because of outdoor operation, the bike is prone to such events.
Repairability	If the frame were to be damaged, it should be easily repaired and not require a change of the entire frame.
Brazing Suitability	For brazing to be an accessible joining process, the chosen material must have a higher melting point than the filler material.

Table 3: Manufacturing considerations.

Method	Pros	Cons	Suitable Base Materials
Soldering	• Low power input and processing temperature • Suitable for joining dissimilar materials • Suitable for joining thin-walled parts • No requirement for post processing heat treatment	• Low strength joints • Not suitable for joining large sections • Joints unsuitable for high temperature applications	Brass, Copper, Iron, Gold, Silver
Brazing	• Low power input and processing temperature • Minimal thermal distortion and residual stresses in joints • No requirement for post processing heat treatment • Suitable for joining dissimilar materials • Strong joints compared to soldering • Stricter control of tolerances since base metal is not melted • Produces corrosion resistant joints • Preserves metallurgical characteristics of base material • Excellent sealing (no porosity for moisture entry)	• Joints not as strong as welding • Not as suitable for high temperature applications as welding • Flux residue needs to be removed • Produces greater thermal distortion and residual stresses	Aluminium, Copper, Gold, Nickel, Silver, Steel

Welding	• Strongest joints • Welded joints more suitable for high temperature applications • Able to join thick and thin sections of metal	• Requires post processing to relieve residual joint stresses • Not appropriate for multi material joining • Welded joints are more brittle	Aluminium, Steel, Titanium
Fasteners	• Cheapest option • Ease of manufacturing • Easy to take apart and replace individual components • Easy to replace fasteners	• Low resistance to shock and vibrations • Joint strength dependent on small fasteners which are more prone to brittle fracture • Not suitable for joining components at an angle	Any

3.4.1 Deriving performance Index 1.

While selecting an appropriate material, it was key to find a balance between stiffness and lightness. Hence, an appropriate performance index must be derived in order to compare various material classes. For simplicity, it is assumed that the frame is loaded like a truss, and each tube experiences a cantilever like load. As a result, the derivation is based on a circular cross section cantilever deflection model as shown in Figure 8.

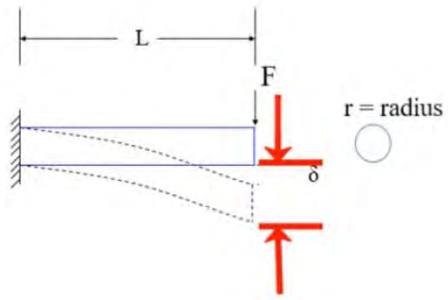

Figure 8: Round Section Cantilever Model (Engineering Materials-Tribology-Design, 2020):

Derivation:

- The performance limiting parameter is minimal deflection (δ), given as:
  - o $\delta = \frac{FL^3}{3EI}$ where I is the area moment of inertia: $\frac{\pi r^4}{4}$
- Substitute expression for I: $\delta = \frac{4FL^3}{3E\pi r^4}$
- Rearrange for radius: $r^2 = \left[\frac{4FL^3}{3E\pi\delta}\right]^{1/2}$
- For lightness, mass must be minimised, given by $m = \pi r^2 L\rho$
- Substitute radius expression : $m = \pi L\rho\left[\frac{4FL^3}{3E\pi\delta}\right]^{1/2} = \pi L\left[\frac{4FL^3}{3\pi\delta}\right]^{1/2}\left(\frac{\rho}{E^{1/2}}\right)$
- A material index $\left(\frac{\rho}{E^{1/2}}\right)$ has been identified and must be minimised to minimise mass (m)
- Performance Index to be maximised: $\left(\frac{E^{1/2}}{\rho}\right) = C$
- Taking Log on both sides: $LogE = 2Log\rho + 2LogC$

Hence, take a performance index line of slope 2 on a $LogE$ vs $Log\rho$ Ashby plot in order to narrow down the classes of suitable materials available, as shown in Figure 9. Additionally, Table 2 summarises the performance of some popular material classes for bicycles. While CFRP is clearly a superior material, the cost to performance ratio is unacceptably high. Additionally, while wood's performance index is good, it has a very low absolute stiffness value. This may not be desirable for efficiently transferring pedal power through the frame.

Table 4: Specific modulus performance of common materials for bicycle application.

Material	Young's Modulus ($\boldsymbol{E/GPa}$)	Density ($\boldsymbol{\rho, g/cm^3}$)	Performance Index $\left(\frac{\boldsymbol{E^{1/2}}}{\boldsymbol{\rho}} = \boldsymbol{C}\right)$	Approximate Cost ($/ton)	Cost to Performance Ratio
Steel	200	7.8	1.81	450	248
Wood	16	0.8	5.0	450	90
Aluminium	69	2.7	3.08	2,000	650
CFRP	200	1.6	8.84	200,000	22,627
Best Material	CFRP	Wood	CFRP	Steel	Wood

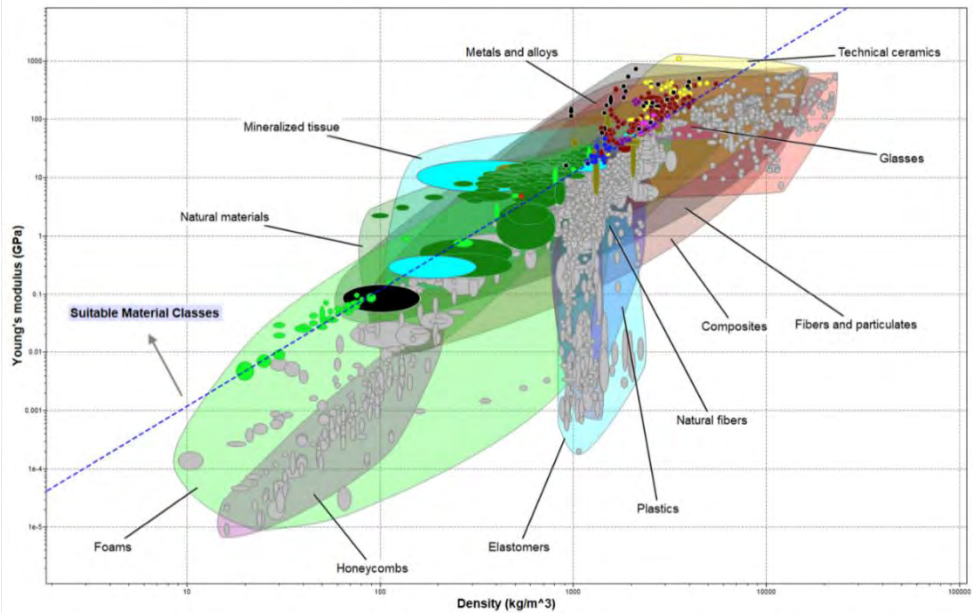

Figure 9: Young's Modulus vs Density.

3.4.2 Deriving performance Index 2.

It was also important to select a material which finds a balance between strength and lightness. The second performance index is also based on the cantilever model in Figure 9.

- Maximum tensile stress for cantilever model found at base: $\sigma = \frac{FLr}{I}$
- Substitute expression for I: $\sigma = \frac{4FL}{\pi r^3}$
- Rearrange for r: $r = \left[\frac{4FL}{\pi\sigma}\right]^{1/3}$
- Substitute into mass equation: $m = \pi r^2 L\rho = \left[\frac{4FL}{\pi\sigma}\right]^{2/3} \pi L\rho = \pi \left[\frac{4FL}{\pi\sigma}\right]^{2/3} L\left(\frac{\rho}{\sigma^{2/3}}\right)$
- A material index $\left(\frac{\rho}{\sigma^{2/3}}\right)$ has been identified and must be minimised to minimise mass, m
- Use yield strength for σ
- Performance Index to be maximised: $\left(\frac{\sigma_y^{2/3}}{\rho}\right) = C$
- Taking Log on both sides: $Log\sigma_y = 1.5Log\rho + 1.5LogC$

Hence, take a performance index line of slope 1.5 on a $Log\sigma_y$ vs $Log\rho$ Ashby plot in order to further narrow down the classes of suitable materials available, as shown in Figure 11. Additionally, Table 3 summarises the performance of some of the most popular material classes for bicycles. In this analysis, CFRP emerges as the highest performance material again. However, given strict budget limitations, it cannot be considered. While wood's performance index is good, it is a difficult material to work with in terms of formability. Even though the

material's cost to performance ratio is desirable, the manufacturing costs associated with wood will be too high.

Table 5: Specific strength performance of common materials for bicycle application.

Material	Yield Strength (σ_y/MPa)	Density $(\rho, g/cm^3)$	Performance Index $\left(\frac{\sigma_y^{2/3}}{\rho}\right) = C$	Approximate Cost ($/ton)	Cost to Performance Ratio
Steel	250	7.8	5.1	450	248
Wood	40	0.8	14.6	450	90
Aluminium	276	2.7	15.7	2,000	650
CFRP	400	1.6	33.9	200,000	22,627
Best Material	CFRP	Wood	CFRP	Steel	Wood

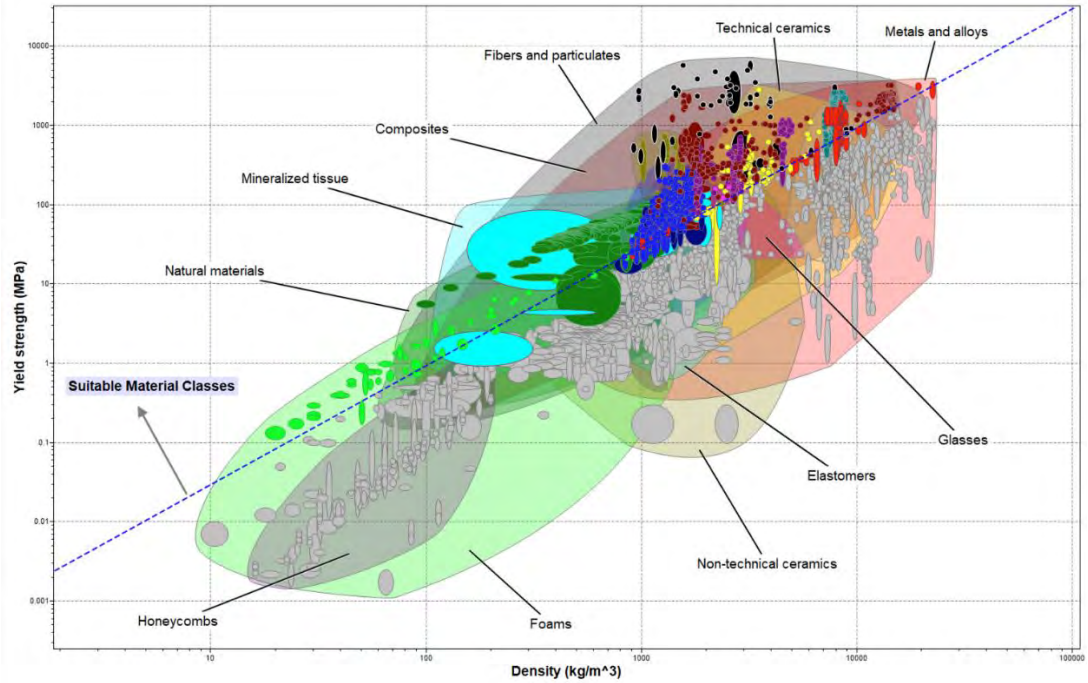

Figure 10: Yield strength vs density.

According to the materials analysis thus far, the most suitable materials to work with are steel and aluminium. While performance is key, the biggest limiting factor in materials selection came from budget constraints and the universe of materials available from actual suppliers. Manufacturing considerations such as brazability and manufacturing costs were also key decision drivers. Table 6 summarizes the materials that were eventually selected for the frame and what their performance scores are.

Table 6: Materials selected for components of the bicycle.

Component	Material Selected	Density ($\boldsymbol{\rho, g/cm^3}$)	Yield Strength ($\boldsymbol{\sigma_y/MPa}$)	Young's Modulus ($\boldsymbol{E/GPa}$)	Performance Score 1 $\left(\frac{E^{1/2}}{\rho}\right)$	Performance Score 2 $\left(\frac{\sigma_y^{2/3}}{\rho}\right)$
Head Tube, Square Sectioned Seat Tube, Down Tube, Seat Stay and Chain Stay Bridges	Mild Steel E220 – Metals4u.com	7.9	220	190	1.74	4.61
Seat Stays, Chain Stays, Inner Seat Tube, Top Tube	Omnicrom – Columbus	7.9	920	179	1.69	11.97
Bottom Bracket Shell	XCR Steel – Columbus	7.9	1000	179	1.69	11.97
Dropout plates	Stainless Steel (304 2B) – Laser Master	8.0	205	190	1.72	4.35
Dropout Inserts, Thru Axle	Aluminium (6082 t651) – Protolabs	2.7 (Aalco,2019)	260 (Alcoa, 2012)	70 (Aalco,2019)	3.1	15.1

Properties for the specialist steels (XCr and Omnicrom) proved difficult to find in their entirety, but a steel exhibiting similar properties was found, using the Cambridge Engineering Selector, in an austenitic AISI 301 steel, ¾ hard (Figure 13). Its Young's Modulus was then used as an approximation to calculate the performance metrics in Table 6. This ensured that when these

materials were joined to build the frame, no weaknesses would occur post-heating. XCr and Omnicrom were favoured due to excellent brazability, high yield strengths and very good resistance to high temperature joining methods.

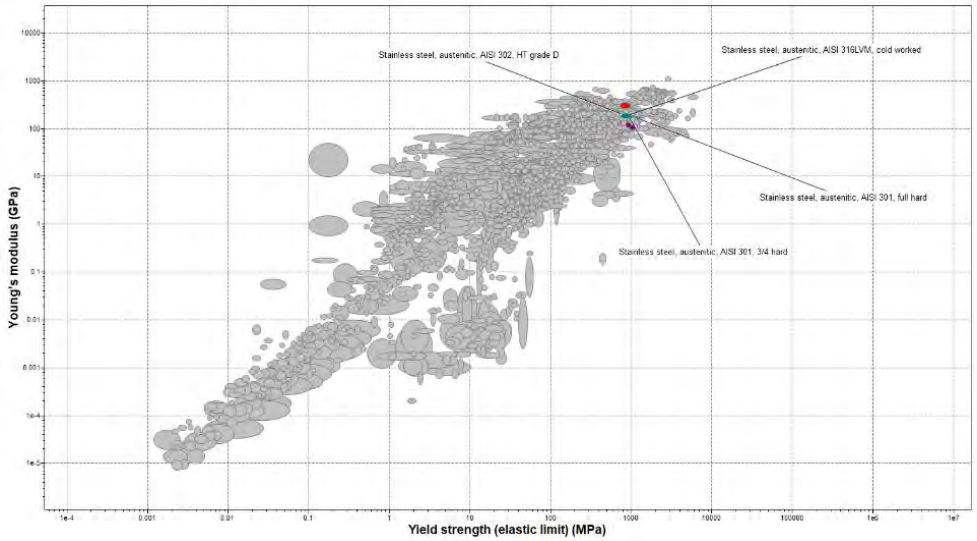

Figure 11: An Ashby map showing the four AISI steels which approximate XCr and Omnicrom's yield strength and joining characteristics well.

Majority of the frame uses varying grades of steel. However, the dropout inserts, and the axle, were identified as critical components, which required higher performance. As a result, aluminium was selected for these components. Overall, the selected materials provide the necessary performance given each of their loading modes while remaining affordable.

3.5 Calculation of stresses along tubes.

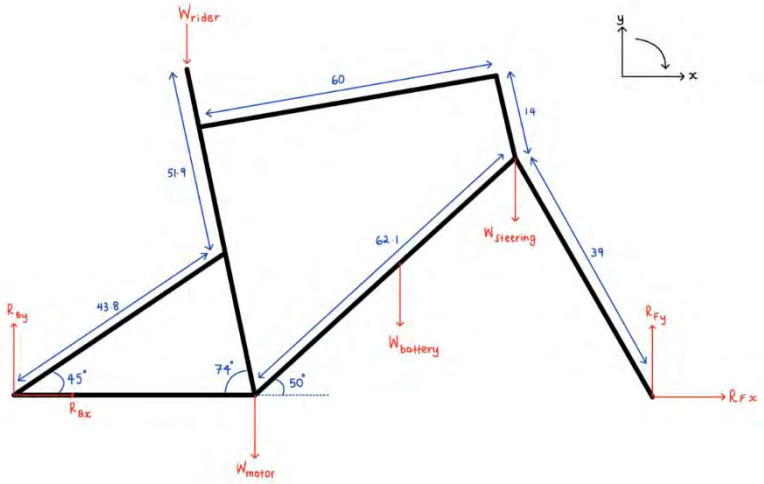

Figure 12: Basic 2 model of frame.

At the very beginning of the project, a simple calculation based on 2-D stress analysis was carried out to find out the order of magnitude of forces along the frame tubes and figure out which tubes are in tension and which are under compression. For tubes under compression, buckling checks were also made to provide a guide for the tube profiles. The seat stays in the concept were identified to be susceptible to buckling.

However, the calculation above is not entirely accurate. With reference to a paper on the stress analysis of bike frames (Covill et al., 2014; C.-C. Lin, S.-J. Huang, C.-C. Liu, 2017), the FEA method is popular, and has been well-adapted in commercial and business fields. So, another stress calculation based on the FEA method was carried out. With considerations that a 3-D model is more complex to create and calculation cannot be done at a high level of accuracy, a 2-D FEA method was used first to give a general preview of stress analysis. This followed the process presented in the ME3 FEAA lecture notes Chapter 3 (Hansen, 2020), modelling the bike frame using five truss elements.

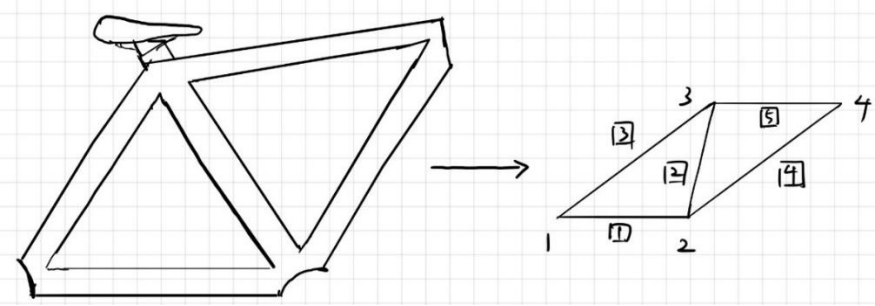

Figure 13: How the frame is converted to a simple model with truss elements.

For each element, several properties need to be determined: the length L, cross-section area A, Young's Modulus E, and the angle of orientation of the element with respect to the horizontal axis θ (represented by d in MATLAB script). Following the steps of the ME3 FEAA lecture notes (Ulrich, 2020), the loads applied at each node were represented by a matrix calculation $\{\boldsymbol{F}\} = [\boldsymbol{k}]\{\boldsymbol{u}\}$, where $\boldsymbol{k}$ is the stiffness matrix and $\boldsymbol{u}$ is the displacement matrix.

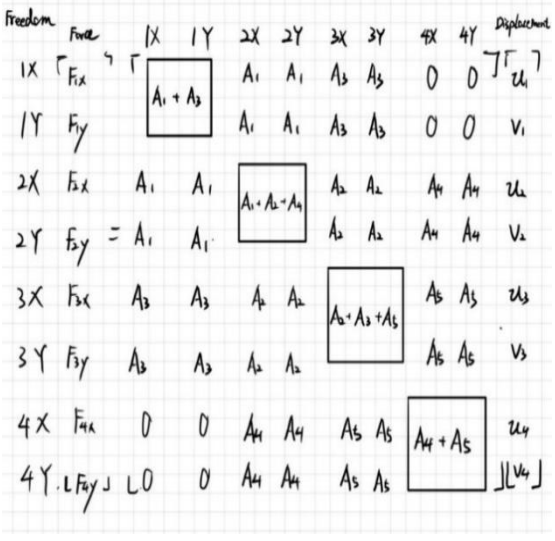

Figure 13: Expanded matrix calculation.

Where ***A*** stands for the contributions from elements with corresponding orders,

$$\boldsymbol{A}_1 = \frac{EA}{L}\begin{bmatrix} c^2 & cs & -c^2 & -cs \\ cs & s^2 & -cs & -s^2 \\ -c^2 & -cs & c^2 & cs \\ -cs & -s^2 & cs & s^2 \end{bmatrix}$$

Where $c = cos\theta$, $s = sin\theta$. The displacements at nodes were obtained by inverse matrix calculation,

$$[\boldsymbol{k}]^{-1}\{\boldsymbol{F}\} = \{\boldsymbol{u}\}$$

The strain in the element was determined by the extension of each element. Since the displacement **u** is known and hence the extension could be calculated. The stresses in the element were directly obtained from strain,

$$Stress = E * Strain$$

The results are as follows:

Table 7: Stresses along tubes.

Element	Stress (MPa)
Chain stays	12.690
Seat tube	-10.051
Seat stays	-17.288
Down tube	7.2308
Top tube	-2.7869

However, through the whole design process, the stresses along tubes need to be checked, and therefore the calculation of stresses must be adjusted and redone for new iterations. To save time and avoid calculating the stresses for every single iteration, a MATLAB script (see link attached in appendix) is created, where all properties for the truss elements were input as matrices, then for the calculation of a new iteration of design only the matrices need to be modified. This MATLAB code simulated three bike riding conditions: normal riding, uphill riding and bumps at the rear wheel. Based on the 2D FEA code simulation results, the viability of our final design is shown to be reasonable since the component elements are all under low displacements and stresses of magnitude of around 10 MPa, which is much lower than the material yield strength (~250 MPa) and a high safety factor can be guaranteed. Regarding the dynamic loads, not only FEA was used to verify the design viability. To ensure the validity of results obtained, several tests were also performed in collaboration with the battery team according to the method previously proposed by Wu in 2013, which showed the maximum upward acceleration under an off-road condition will be around 8g for a short moment, under which a safety factor of over 2 can still be maintained.

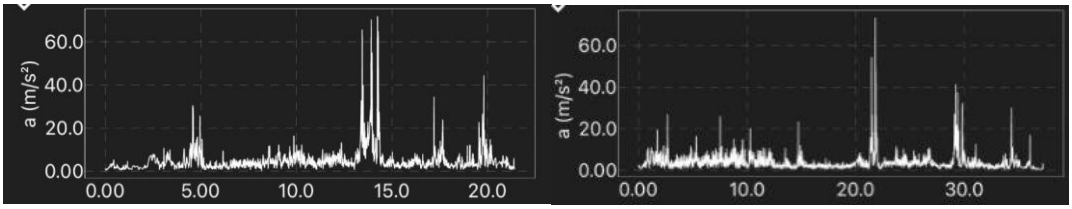

Figure 14: Fig. upward acceleration monitored at a bike frame under off-road conditions.

3.6 Frame Redesign Phase 1

Simple 2D stress analysis methods mentioned in Section 3.5 identified potential buckling zones in the seat stay region. The initial concept model also presented numerous other potential problems, with stress concentrations caused by sharp corners in the battery slot being the major concern. Furthermore, manufacturing methods and material selection as previously mentioned were yet to be considered into the design. The second major iteration of the design solved some potential problems from the first iteration. It no longer had sharp corners, and the previous method of motor integration was changed into mounting with a yet unknown battery mounting method. As requested by the motor team, it had standard bottom bracket compatibility. In terms of material selection, Aluminium 6082 was chosen based on market availability. However as highlighted in Figure 15, the design still showed problems.

Figure 15. Second iteration of frame design annotated with remaining problems.

Specifically, the seat-stays and chain-stays required curved profiles to avoid pedal crank interference, and precise geometry was needed for the seat post tube to accommodate a standard bike seat post. To produce these parts would have required extrusion or extensive forming, which are far beyond the budget considerations of this project.

Additionally, concerns from other subgroups were raised simultaneously. Due to the aluminium construction, weldability of external sub-assemblies could be limited, especially if different non-specialist manufacturers were used. From the steering team, a decision to persist with disc brakes rather than rim brakes set up an interesting design challenge and proved to be a turning point in the design phase.

3.7 Rear Dropouts Design and Disc Brake Specifications

Designing a system to accommodate for a chain tensioning mechanism as required by the motor team while also housing disc brakes turned out to be more difficult than expected. Significant time was spent on optimising this component for functionality, structural properties, and cost. There is a dual challenge in being able the slide the entirety of the rear axle and the wheel, while ensuring the disc brake rotor remains in line with the wheel. Four solutions were considered for this: a tensioner, a spring-loaded tensioner, an eccentric bottom bracket and sliding dropouts. Tensioners have the disadvantage of chain slippage and jumps if riding on rough terrain or if sudden bumps are encountered. Eccentric bottom brackets were ruled out due to their incompatibility with the gearbox assembly. Sliding dropouts were the only design that did not clash with any other requirements. They introduced the possibility of moving the disc rotor alongside the rear axle. Like the initial stages of frame design, extensive research on existing sliding dropout designs was performed. However, resources revealing relevant design details were scarce. Engineering drawings of sliding dropouts from Paragon Machine Works(Paragon Machine Works, n.d.) proved to extremely helpful. A CAD recreation of the drawings helped with visualising the mechanism as shown in Figure 18.

Figure 16: Estimated CAD recreation of commercially available sliding dropouts by Paragon Machine Works, assembled on the rear wheel with disc brake callipers attached.

Due to the lack of availability of the product in the UK, the team decided to the pursue the design regardless by designing the dropouts from the ground up. This revealed another opportunity to tailor the design specifically to the team's requirements. The team also took on the responsibility of choosing disc brake mounting. Before designing the new sliding dropouts, it was necessary to understand the differences between the three-disc brake mounting standards: ISO, Post mount and Flat mount.

3.8 Frame Redesign Phase 2

To work towards manufacturability, the team decided to start from scratch. During the meeting with the Bicycle Academy, who were approached for a quote on manufacturing the frame, a software named BikeCAD was recommended as it is commonly used across the bike industry. Later on, a bespoke design for the rear dropouts was made.

3.8.1 Three part Sliding Dropouts Design

To transmit braking forces to the frame more effectively, the brake calliper had to be mounted parallel to the chain stay and have multiple connecting faces to the chain stay to minimize pivoting. Shimano's flat mount brake calliper standard (Pverdone, 2018) (Section 8.4) allowed this to be done within the smallest overall footprint, thus reducing material in the dropouts.

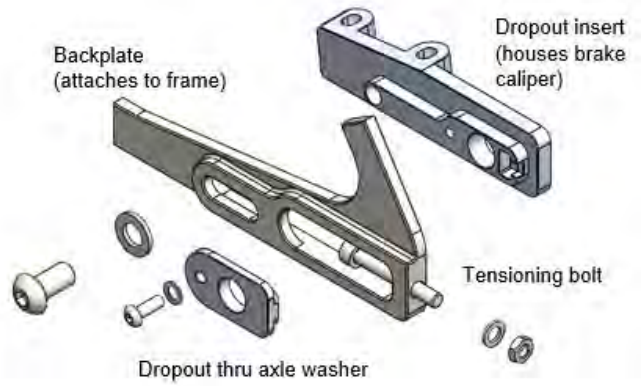

Figure 17. Final left dropout assembly

3.8.2 Wheel attachment method

Conventionally, 10mm quick release skewers are used to secure the wheel. However, designing to the specification criteria of a 30kg bike, a stiffer 12mm THRU axle design was found to be more appropriate. This featured a 1.5mm pitched thread on one end, where the axle would go through the left dropout and screw on to the right dropout as shown in Figure 18. Having decided on a 700cc wheel, designed to fit 10 speed hubs, with the steering team, the effect axle

length (inner face to inner face of the dropouts) was fixed at 142mm. However, using custom sliding dropouts added some complexity as the spacing between the two outer faces of the dropouts were wider than available standard thru axles and necessitated a custom design.

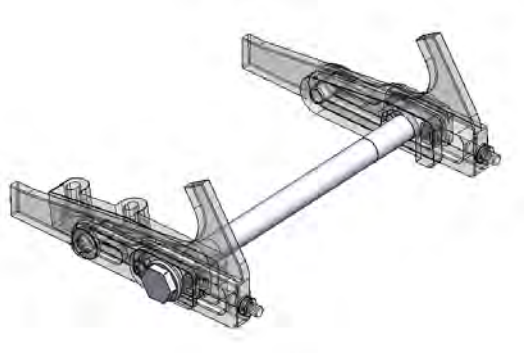

Figure 18. Designed thru axle secured between the two dropouts and the rear wheel hidden.

3.8.3 Considering Rider Anthropometrics

The redesign was an opportunity to tailor the frame geometry to the target user. As shown in Figure 19, this software considers anthropometrics when designing the frame. It allows users to input various parameters of both the bike and rider. The previous design had a standard road bike silhouette which is more targeted towards achieving greatest speeds rather than providing comfort. However, for a city bike, comfort was deemed key and altering the frame geometry was an easy way to achieve that. BikeCAD was used to verify the new layout of the frame, due to its ability to suggest more appropriate geometries.

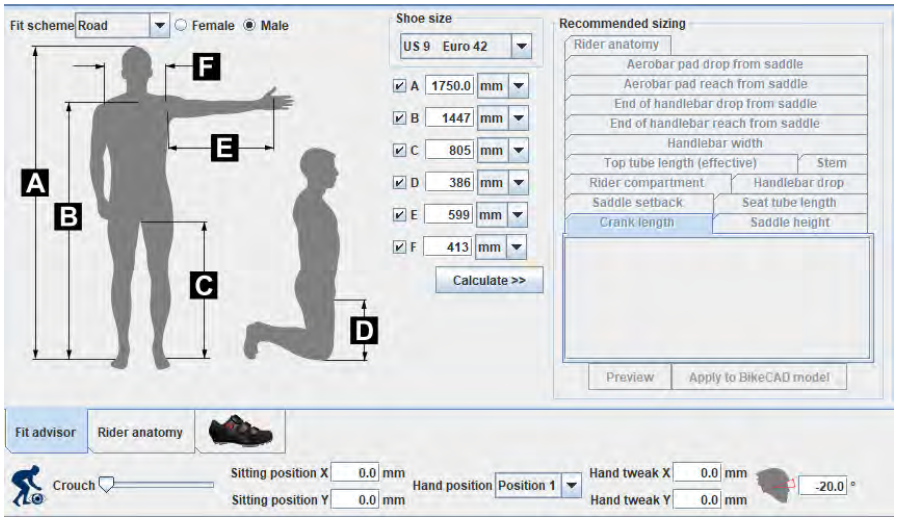

Figure 19: A screenshot of BikeCAD.

3.8.4 Frame Tubing

To overcome the supply and welding issues faced with using industrial grade Aluminium tubes, bicycle frame-specific steel tubing from Columbus was used for the design. On top of this, the butted profile saves weight by only having required thicknesses in areas of weld joints. The selected tubing from the Columbus catalogue (Columbus, 2020) is as summarized in Table 8.

Main Tubes:

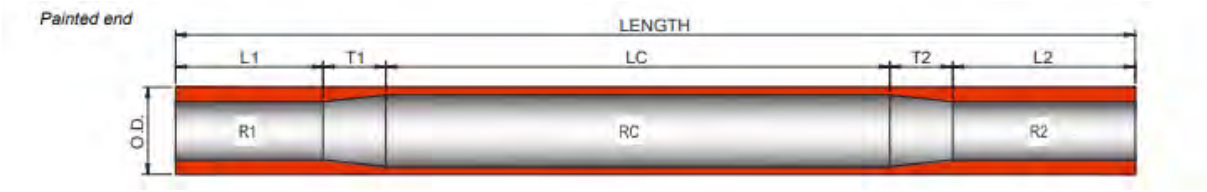

Table 8. Selected Columbus Steel Tubing

Part	Code	O.D.	Length (mm)	Thicknesses (mm)			L1 (mm)	T1 (mm)	LC (mm)	T2 (mm)	L2 (mm)	Family
Downtube	SLFL12650	35	650	0.65	0.45	0.65	60	40	390	40	120	Spirit HSS
Toptube	SLFL11560	31.7	560	0.65	0.45	0.65	40	40	340	40	100	Spirit HSS
Seattube	SLFI3560	28.6	560	0.75	0.4	0.6	130	30	210	30	160	Life

3.8.5 Proposed Mounting Solutions

The second iteration featured all bicycle-specific tubing with circular profiles. The subassemblies were proposed to be attached on to the frame using welded inserts as shown in Figure 20.

Figure 20. Phase 2 redesigned assembly with proposed motor plate mounting tabs.

3.9 Design of first iteration for manufacture.

The following section details the final design and shows the final inter-group design. While the design ultimately did not change significantly from the phase 2 redesign, the mounting method for other sub-assemblies was reconsidered. Large flat surfaces were required for direct brazing of the motor plate and seating the battery bracket. This was achieved by replacing the seat-tube with a hybrid design containing the shortened original seat tube with a square steel sleeve. Similarly, the downtube was replaced with a square-profiled tube.

Figure 21: Final intergroup-assembly render.

The dropouts were initially designed to be CNC milled from Stainless Steel and Aluminium, but costs for this were prohibitively high. Thus, alternatives were pursued, and an updated design was employed.

Quotes from Tridan and MRT Castings (as an estimate) cost £2700 and £925 respectively, excluding VAT. A third supplier, Protolabs, put the cost at £1016.58, excluding VAT. The design was changed, as a contingency, as it was unlikely that the high price would be acceptable to the department. The design was simplified by removing the steps on the thin surface of the part, and smoothing the edges both to remove features which were difficult to machine, and to make the design easier to hold in the clamps of CNC mills. The main plate of the dropout was the most expensive component, at £685 each from Tridan originally, and £250 each from MRT Castings (for both the left- and right-side). There was a significant reduction in price between these quotes, but the components remained very expensive. The alternative proposition was to manufacture the dropout in two parts and join them together. This allowed both halves of the dropout to be cut from sheet steel, using either waterjet or laser cutting, and then joined, which would remove some of the complex features and make those individual parts cheaper to produce. It mitigated the costs of manufacturing bespoke left- and right-sided components,

making the parts mirror-images of each other and identical until joined. Waterjet cutting and laser-cutting workshops were contacted. TMC Waterjet quoted costs of £210, including VAT, but excluding joining. This included a £100 material cost, and the company recommended laser cutting as an alternative. Other quotes ranged from £82.83 from Accurate Laser Cutting to £30 from Laser Master (both including VAT). This included the material cost but not joining of the two parts. Laser Master then produced a quote including the joining of the components for £180 on top of the machining costs, including VAT. The gross costs of both dropout plates was now £210, a significant reduction compared to previous quotes. The inserts were still to be CNC machined, at the costs prescribed by Protolabs, but this change lowered the cost significantly.

3.10 Manufacturing overview

The manufacture of the frame has been outsourced to workshops this year in accordance with the module requirements. Given that the joining facilities within the STW are not available for use, it was undertaken to have the frame joined by an external workshop, as required. The manufacturer which was selected to perform this task was The Bicycle Academy. This manufacturer was also able to provide the jigs which would hold the frame in its required shape when joining. This provides security that the frame will be joined as specified by our design. When the dropouts are attached to the rear of the bike, they are constrained by use of a jig representing a dummy axle, to maintain their concentricity. These jigs ensure that the frame will be correct in its dimensions once joined. The prospect of deformation during the joining process (due to heating) is mitigated by the jigs. The dropouts are to be manufactured in parts. The main plate of the dropouts, which attaches to the seat stay and chain stay, is to be laser-cut in two parts from sheet stainless steel and joined. The inserts for the dropouts will be CNC machined, and then are inserted into the dropout plate and secured with bolts, which will allow them to slide. The right-side outer component of these inserts on the dropout is to be threaded, in the STW, such that the thru axle can bolt into it. The thru axle is to be CNC turned from aluminium bar and threaded such that it tightens into the right-side nut, the outer component. This stationary thru axle then supports the rear wheel hub, which contains the bearings for the wheel.

3.11 Design for manufacture

A significant component of the redesign of the dropouts included changes to promote manufacturability. Initially, rounded edges on the components and multiple steps on a thin part would have led to a high number of tool passes during CNC machining, and tight corners and small features on the parts would have left material that was unable to be removed. The

rounded edges gave way to squared-off ends, which had a dual benefit of making the part less complex to machine and providing tabs by which the part could be fixed in the clamps of the CNC mill during the process. The stepped profile on the front of the part was removed and the thickness increased, which reduced the number of operations needed to achieve the required dimensions.

3.12 Simulation

3.12.1 Simulation analyses

As CAD files were generated during the design, analyses were undertaken to assess the strength of the frame for the exact geometries of its components and under the loads put on it by other subassemblies. This was an iterative process and was repeated as the design evolved between versions to ensure that the measurements of the frame's strength could be kept up to date. As per the Quality Plan, Abaqus CAE was used at first. This involved the conversion of the Solidworks parts and assemblies to .igs files, and presented difficulties with meshing the shells which represented the butted tube sections of the frame. As a solution to this, Solidworks Simulation was chosen as an alternative software.

An initial simplification was made, taking g = 10.0 ms^{-2}, both to increase the ease of analysis and to provide an upper estimate of the stresses experienced by the frame.

This was refined as more exact mass data was gathered from each subassembly.

Another initial assumption was taken that the frame would be able to support its own weight in the analysis, and so its weight was not included. Given that the final mass of the frame indicated by Solidworks with materials populated is 5.9 kg, this is seen as a reasonable assumption.

It was hoped initially that analysis might include the frame along with all subassembly components in full. However, this led to extremely large file sizes and long computation times, due to the meshing requirements across the many different components. It was deemed sufficient to analyse only the frame, rather than including every subassembly – instead, their masses on the frame and any constraints that would have been present, were substituted in.

3.12.2 Initial analysis.

The primary analysis which was undertaken was comprised of the old frame design. The whole welded structure of the frame was included in this simulation (the tubes and dropouts), and components such as the wheels and saddle / seat post were excluded. This decision was taken to increase the efficiency of the analysis (reducing file sizes and the computational and time requirements for meshing), and because the components on the frame which had been

purchased from external suppliers were assumed to be of sufficient strength that further analysis on them was not required.

The loads on the frame were updated throughout the course of the analyses, and initially the distribution was taken to be as follows. An 800 N force was applied to the top section of the seat tube to simulate the weight of the rider. A 100 N force was applied through the head tube to simulate the component of the rider's weight on the front of the bike and steering assembly, an 80 N force represented the weight of the motor, acting downwards on the join between the top tube and seat tube, and a 50 N force on the down tube represented the weight of the battery. Within this simulation, the effects of gravity were also included. The constraints on the frame were assumed to be as follows; the dropouts were fixed in position to simulate their attachment to the rear axle, and the base of the headtube was fixed in position to simulate its support by the headset assembly. The analysis yielded positive results, showing maximum displacements on the order of 0.1 mm (at the seat post tube).

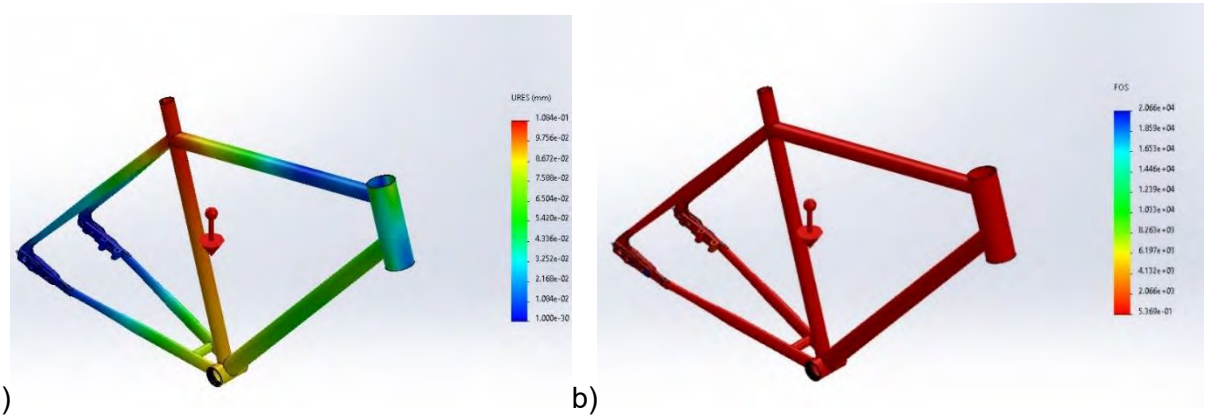

a) b)

Figure 22: a) A displacement plot of the initial analysis of the frame (maximum value 0.108 mm). b) A safety factor plot of the initial analysis of the frame (minimum value 0.54).

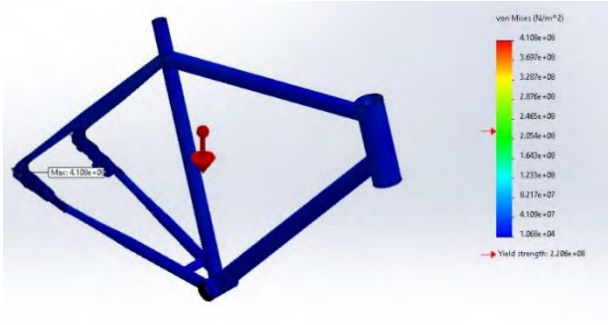

Figure 23: A von Mises stress plot of the initial analysis of the frame (maximum value 410 MPa).

The design shows a minimum factor of safety of 0.54, and a maximum stress of 410 MPa. This is shown to be significantly above the yield strength, which initially appears very discouraging. However, the simulation presented an issue as it ran, which is explained briefly here.

When the simulation was performed, the bolts within the dropout assembly were converted to connectors within the simulation. Solidworks notes that in some simulations using these connectors, a significant stress concentration can occur around the bolt holes (which would not otherwise be present). This is shown in Figure 24:

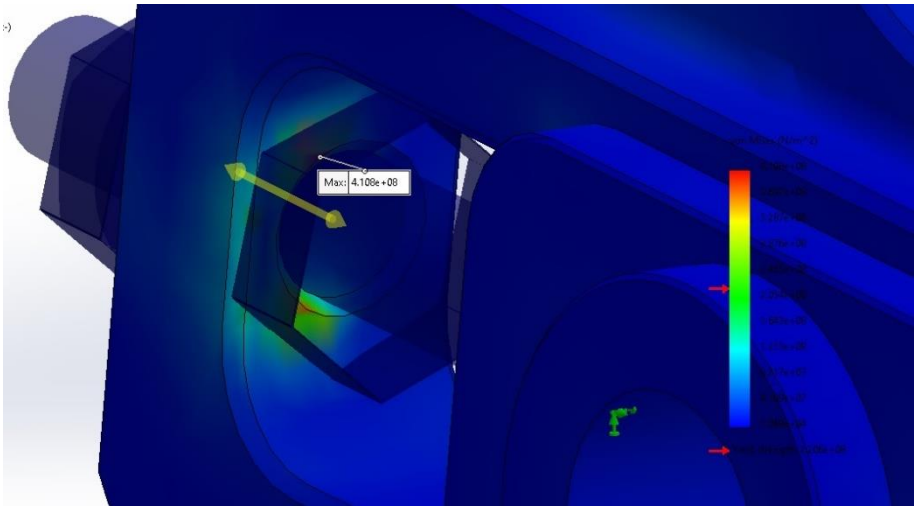

Figure 25: A von Mises stress plot at the right dropout, showing the stress concentration around the bolt connector hole.

As can be seen from the contours in the stress plot, the image is zoomed in on the rear of the dropout, where the hole for the tensioning bolt is. The simulation has predicted a stress of 410 MPa at this point, which is not backed up by either the displacement plot (above) or the strain values (below), which show the strain exhibited within the frame to be very small (with a maximum of 0.0012 mm). This, combined with the prior warning from the program about the accuracy of the stresses at such connector holes, serves to permit the classification of the spike in stress as an anomaly. This led the conversion of these bolts to connectors to be discontinued in further simulations.

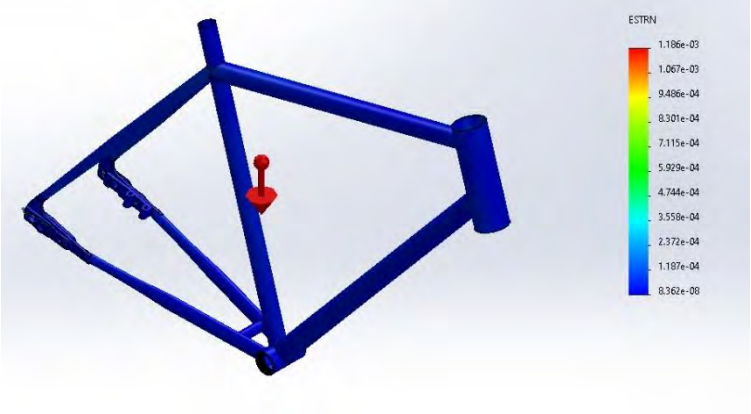

Figure 26: A strain plot of the old analysis of the frame.

3.12.3 Interim analysis; post-redesign. FEA iteration 1.

After discussion with both the group's supervisor and other groups and their supervisors, and adding in the box section tubes to the frame, analysis was undertaken once more to assess the validity of the updated design. The distribution of loads was kept the same, but the positions of the loads were updated slightly to reflect the mounting positions of the subassemblies. The motor plate is to be welded to the right-hand side of the square section of the seat tube, and so its weight force was applied there. The battery was to be mounted in the same position as previously expected, but the assignment of the weight force was updated to sit on the top face of the down tube. The frame was constrained at the dropouts, using a fixed constraint, which was later updated to a hinge. Updating the constraint was necessary to more accurately reflect the boundary conditions encountered by the frame when riding (since the dropouts could not be assumed to stay fixed), but these fixed constraints did also provide a useful sense check (in line with the constraints advised in the testing procedures from BS EN15194-2017), so the results of these analyses were kept and are shown below.

Figure 27: A safety factor plot of the interim analysis of the frame (minimum value 2.8).

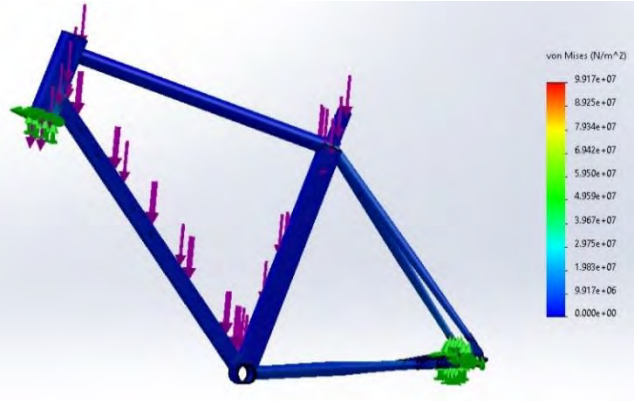

Figure 28: A von Mises stress plot of the interim analysis of the frame (max value 99 MPa).

3.12.4 Final analysis

A variety of constraints were used for this analysis. One was to constrain the rear axle in a fixed, and then a hinge configuration. This permitted simulation of the frame under loading both with the dropouts clamped, and as if the rear wheel assembly were present (fixing the height of the axle and allowing the dropouts to pivot about it). The update of the constraint at the rear axle and dropouts was necessary, since the hinged constraint provided a better approximation of the loading of the bike in operation than simply fixing the dropouts' position. The base of the head tube was put on roller mounts, an improvement over simply fixing its position in the assumption of being supported by the headset and front fork, since it was free to move horizontally, should the front wheel move as the frame is loaded. The most up-to-date masses of each assembly were used. These are shown in Table 9 below, as are applied forces in Table 10.

Table 9: Components and masses.

Subassembly	Mass (kg)
Motor	8
Steering	7
Battery	4.3
Rider	80

Table 10: Forces applied to the frame.

Name	Force	Location
Weight of rider	80g N (784.8 N)	Applied vertically downwards to top of inside face of seat tube.
Weight of battery	4.3g N (42.183 N)	Applied vertically downwards to top face of square down tube.

Weight of motor	8g N (78.48 N)	Applied vertically downwards to right-hand side of seat tube square section.
Component of rider weight through steering assembly	100 N	Applied vertically downwards on inside of the head tube.

The mass of the steering assembly was not incorporated into the analysis due to the constraints applied; it can be considered that the support from below the headtube is the vertical support of the front wheel and fork, and that the load of 100 N on the head tube includes both the component of the rider's weight through the handlebars and the weight of the internal components of the headset assembly (since during normal, seated riding such as a commute on this bike, downward force is not significantly applied to the handlebars by the rider).
The final analysis, using the most up-to-date weights and constraints, yields a minimum safety factor of 1.1. This is concentrated at the cut in the seat stay, where the dropouts are inserted, as shown below.

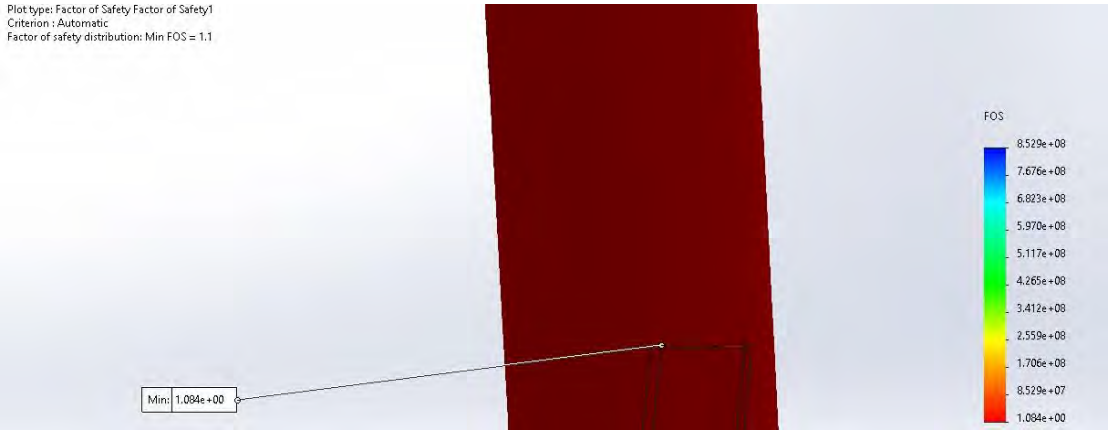

Figure 29: Screenshot showing minimum safety factor at dropout-seat stay interface.

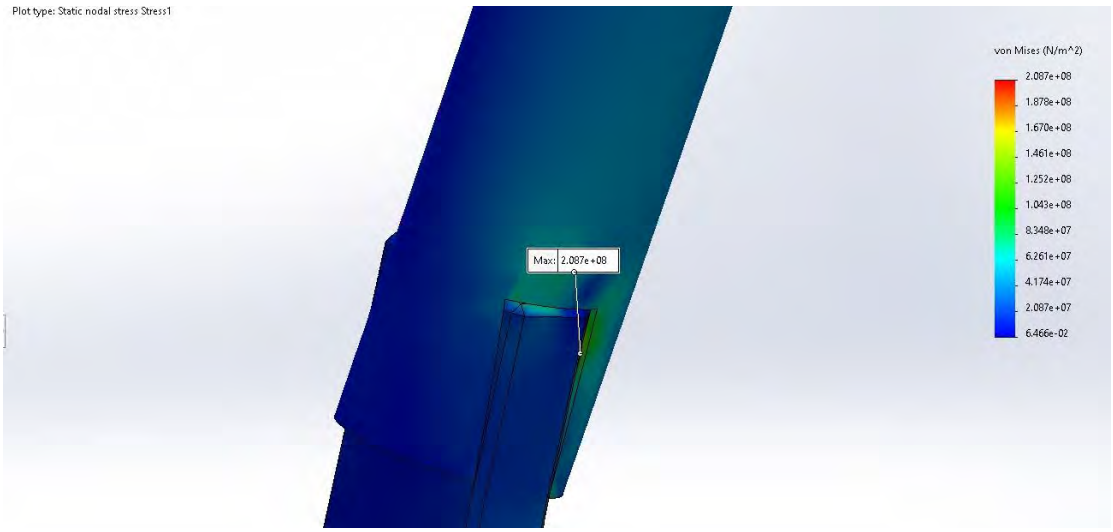

Figure 30: Screenshot showing stress concentration factor at dropout-seat stay interface.

This result will be further discussed in Section 5.1. The frame performed well in this test, exhibiting generally very low stresses within all components. The low safety factor stems from the stress concentrations which occur around the dropouts, and the headtube. At the dropouts, as shown in the plot above, the stress increases around the cuts made for the dropouts. Figures *Figure 29*,*Figure 30* (above) show the minimum safety factor and maximum stress occurring where the dropout meets the seat stay. The locations of these stress concentrations are to be expected, and further concentrations occur around the headtube and at cut ends of the tubes, as would also be expected. The average and root mean stresses were recorded for the assembly. The root mean stress was found to be 4.994 MPa and the average stress 3.083 MPa. These values agree with the orders of the stresses found within the beams of the 2D analysis in Section 3.5, indicating that most of the stresses on the frame do not significantly exceed 10 MPa.

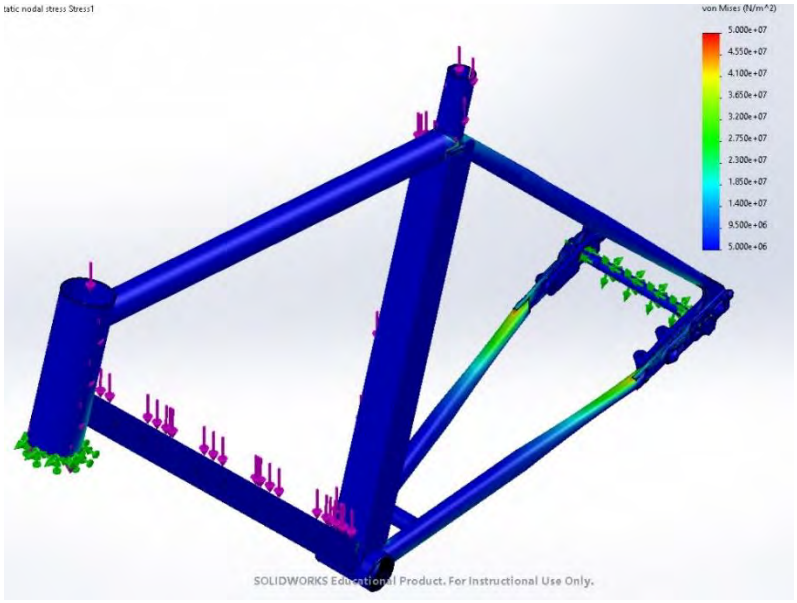

Figure 31: A von Mises stress plot of the frame, showing areas of stress concentration.

Another important component for the analysis of the frame were the dropouts. These were analysed both with and separately to the frame to assess their suitability. The steel central plates, and subsequently the dropout subassemblies, were analysed, as illustrated in FiguresFigure 32,Figure 33 and Figure 34.

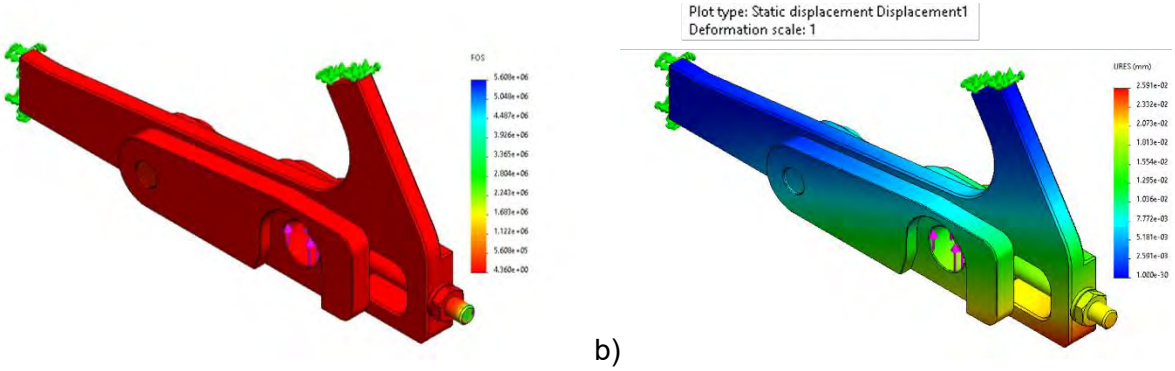

a) b)

Figure 32: Plots of the right dropout assembly, showing a) safety factor (minimum value 4.4) and b) displacement (maximum value 0.026 mm).

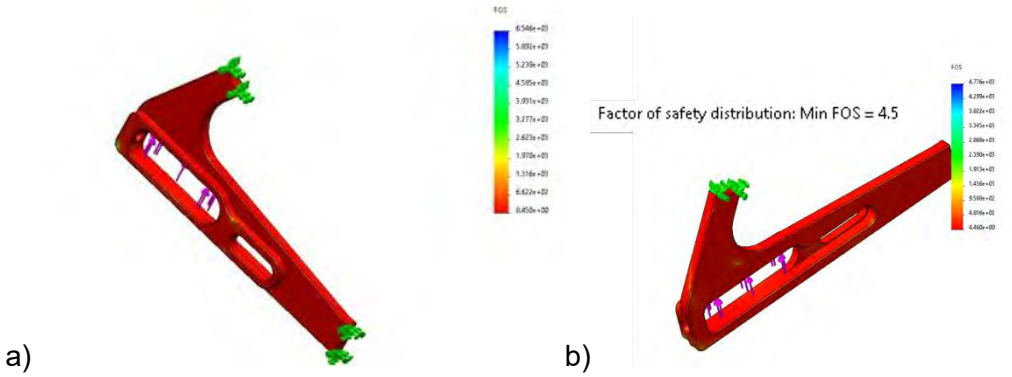

a) b)

Figure 33: Safety factor plots of a) the right dropout plate (minimum value 8.5) and b) the left dropout plate (minimum value 4.5).

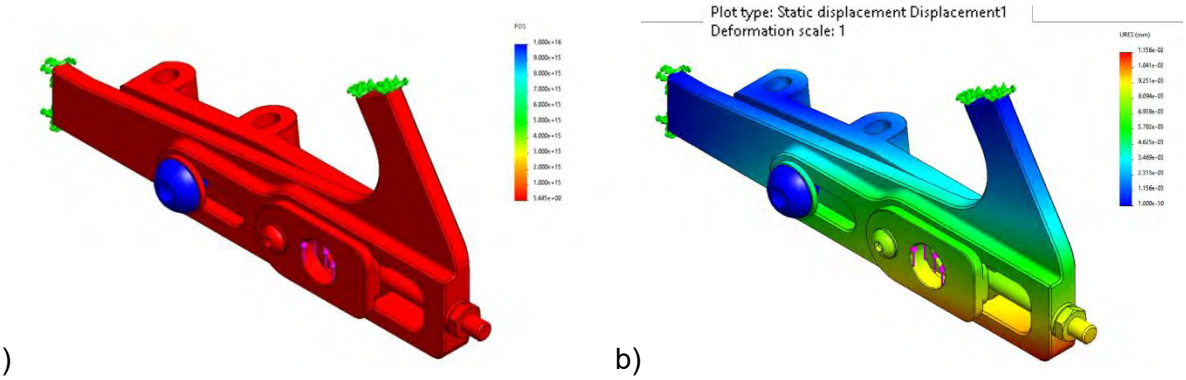

a) b)

Figure 34: Plots of the left dropout assembly, showing a) safety factor (minimum value 5.6) and b) displacement (maximum value 0.016 mm).

The dropouts were taken to experience an upward force of 300 N each as reaction from the wheel and axle. This was taken from the assumption of the whole bike and rider combined having the maximum predicted mass (110 kg), which was then taken (using g = 10 ms^{-2} once more for an increased factor of safety) to be an 1100 N weight force. The distribution of this force was assumed to be biased towards the rear of the frame, given the rider's position on the saddle, and so 600 N of the weight force would be applied through the rear wheel, for the purposes of this analysis. Resolving forces vertically, this provided the 300 N reaction force value acting through each dropout. This 300 N force was then applied vertically upwards on both the central dropout plate and the whole assembly in subsequent analyses, with the assumption of fixed constraints at the welds to the chain stays and seat stays.

The dropouts themselves performed very well, as did the dropout assemblies. Upon completing the simulation, the results shown above were obtained. These indicate that the stresses within

the dropouts and the inserts were sufficiently low to ensure a minimum safety factor within the left and right dropout plates of 4.5. When this was extended to the assemblies, the minimum safety factor was 4.4. These results provide confidence that the dropouts will perform well under normal riding loads. FEA of the axle was also undertaken to check that it met the required safety factor. The analysis which was performed used a constraint at the location of the dropouts on the axle, so it was fixed as it would be when attached to the bike. The equivalent force to that placed on both dropouts (600N, through the rear wheel) was taken to act down through the area of the axle which was covered by the hub. This showed a minimum safety factor of 4.1, above the design specification value, as in Figure 35.

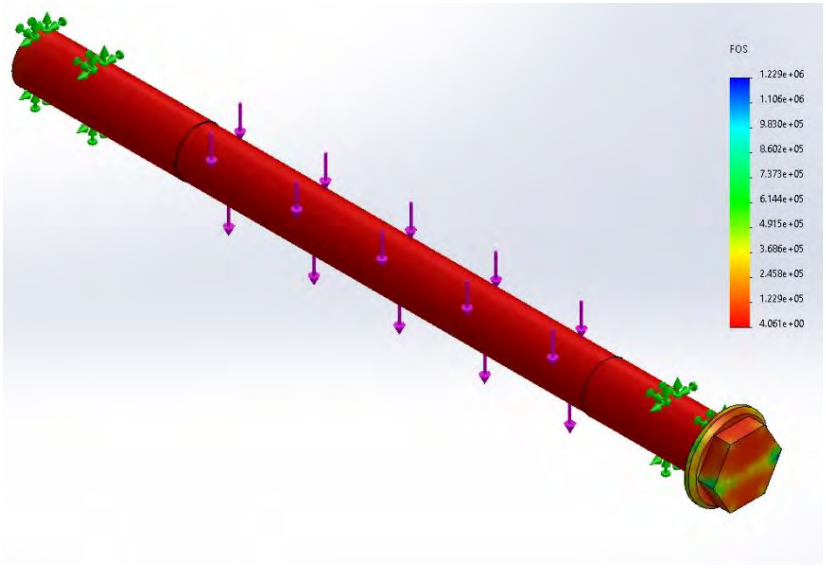

Figure 35: A plot of the rear thru axle, showing the safety factor (minimum value 4.1).

The stress across the rear axle was also obtained by hand calculation based on beam theory to verify the simulation results. By assuming a two-side constraints model, the end moment M and stress are given by,

$$M = \frac{WL}{8} = \frac{600 * 0.12}{8} = 9Nm$$

$$\sigma = \frac{My}{I} = \frac{9 * 0.006}{1.018 * 10^{-9}} = 53\ MPa$$

Which shows a safety factor of approximately 4.7.

Overall, the FEA simulations which have been performed give the team an indication that the frame will perform well under loads experienced during riding, as demonstrated by the generally high factor of safety, and the low stresses present when the frame is simulated in accordance with the rider weight specified in the PDS, and the loads from the masses of each subassembly.

3.13 Manufacture methods chosen

The manufacture methods which have been chosen for the frame are as follows: CNC milling is to be used to cut the dropout inserts. CNC turning is to be used to make the axle. The main plate of the dropouts will be produced by laser cutting, and then joined and the tensioner hole will be bored. The frame will be brazed together, from tubing which has been cut to size and to angle, using a for-purpose bicycle welding jig configured by the frame builder.

3.14 Alternative methods considered

CNC milling was initially considered for the central dropout plates, as well as the inserts. Due, as described, to the high costs incurred for such a component, the alternative design detailed above was pursued. Furthermore, an alternative quote for the revised design of the dropout plates was obtained from Protolabs (for CNC machining these components), which came at a cost of £832.33 including VAT. This was significantly higher than the cost Laser Master provided and did not include joining. This led CNC of the dropout plates to be disregarded. Waterjet cutting was also considered for the dropout plates (recommended laser, cost too high for quote received).

3.15 How the Manufacturing Readiness Review influenced plans

Feedback from the Manufacturing Readiness Review included questions about the mounting of other subassemblies. Ideas were in place, for example; welded tabs which would connect the motor plate to the frame, as used on dirt bikes, but this was refined after the MRR. After further discussion with the motor team, as a result of this feedback, the decision was taken to introduce square sections into the downtube and the seat tube, which allowed the motor team to weld the mounting plate directly to the side of the bike and also increased the ease of mounting the battery. Mechanical mounting of components was suggested by the assessor. It was decided not to include this feedback entirely, since the motor team were opposed to the fastening of their mounting plate to the frame, instead strongly preferring joining as a permanent, integrated method. The battery, however, was fastened to the frame using bolts because of the redesign prompted by the feedback in the MRR, which satisfied the suggestion of the use of fasteners where appropriate. It also led to the battery being non-removable, as per the original brief and overall group PDS. The frame, motor and battery subassemblies collaborated on mounting-since it was necessary to determine where these assemblies would fit together.

4 Design verification plan

4.1 Testing Methods Iteration 1

The initial approach to testing involved following British Standard guidelines for EAPCs. Five tests were selected based on their ability to describe the impact and fatigue performance criteria laid out in the Product Design Specification.

4.1.1 Testing Resources Considerations

While the ideal scenario would be to replicate British Standards compliant testing procedures, the tests are limited by available testing facilities and budget constraints. Table Table 11 is a summary of the required resources, testing facilities and their respective budget impacts.

Table 11: Required facilities and resources and their impacts on the budget.

Required Facilities and Resources	Budget Impacts
5 x Dummy Forks	High
1 x Fixed Roller	Low
1 x Dummy Seat Post	Med
1 x Locked Suspension Unit	Med
1 x Dummy Crank Replacement	Med
3 x Loading Masses	Med
1 x Vertical Link	Low
1 x Striker Mass	Med
8 hours 50 mins of Technician Time (£50/hr)	£442

Due to a highly constrained budget, a fully compliant set of test procedures did not seem viable. The procedures were also arduous and time consuming. Furthermore, complete testing required visible deformation and cracks in the frame. Since there was insufficient budget to manufacture a second frame, damaging the original assembly was not ideal. Furthermore, permanent damage will leave other sub-assembly groups without a functional frame to work with. As a result, a second iteration of testing procedures was considered.

4.2 Testing Methods Iteration 2

Three test options were considered:

1. **Dummy Component Testing**: Identifying the most vulnerable sub-assemblies in the frame, recreating dummy components matching their mechanical properties then destructively testing them.

2. **Non-destructive Testing**: Test the original frame assembly at a fraction of the failure stresses, then measure elastic deformation using strain gauges or extensometers.
3. **Fracture Modelling**: Test the original frame till crack formation, then model the required stresses for the crack to grow till a length sufficient to cause complete rupture.

In order to select one of these methods, a testing decision matrix was created.

4.2.1 Testing Decision Matrix

Test Name	Pros	Cons
1. Dummy Component Testing	• Models the stress concentrations well • Can be tested destructively • Does not require the large and complex rigs that a full frame assembly would require • Protects original frame from any damage • Cheapest option • Easiest testing method	• Relies on FEA modelling to identify highest stress components • Requires brazing and cutting to replicate similar stress concentrations • Not a test of the full frame assembly • Requires additional manufacturing and material
2. Non-destructive Testing	• Protects original frame from significant damage • Saves costs associated with destructive dummy component testing • Tests the full frame	• Introduces no failure in the frame • Overly reliant on calculations and models • If FEA models are not accurate, risk of accidental and irreversible damage to original frame • Difficult to define fraction of stresses to be applied • Requires as many testing resources as iteration 1

3. Fracture Modelling	• Does not require additional components for fully destructive testing • Introduces some failure which allows for a higher safety factor than non-destructive testing • Tests the full frame	• Damages original frame • Fracture modelling cannot fully replicate real crack propagation, which can be affected by additional thermal or residual stresses that are difficult to model • Requires as many testing resources as iteration 1

To protect the original frame while testing as accurately as possible within budget, *Dummy Component Testing* was selected. This test method was also eventually approved by the project Supervisor.

4.3 Dummy Component Testing

4.3.1 Selecting Test Components

Successful testing using this method relies on careful and accurate selection of the components to test. To identify the likely points of failure, Finite Element Analysis (FEA) was adopted. Figure 36 shows an analysis of the frame assembly under static stresses during normal loading conditions. The forces come from the weight of the rider and the remaining bicycle. The table below summarises the expected failure modes.

Component	Expected Failure Mode
1. Chain stays + Dropouts	Rider Load Fatigue
2. Seat stays	Rider Load Fatigue
3. Box Section Seat Tube	Rider Load Buckling
4. Brazed Joint on Bottom Bracket	Pedalling Fatigue
5. Top Tube	Collision Impact Fracture
6. Down Tube + Head Tube	Brazed Joint Pedalling Fatigue

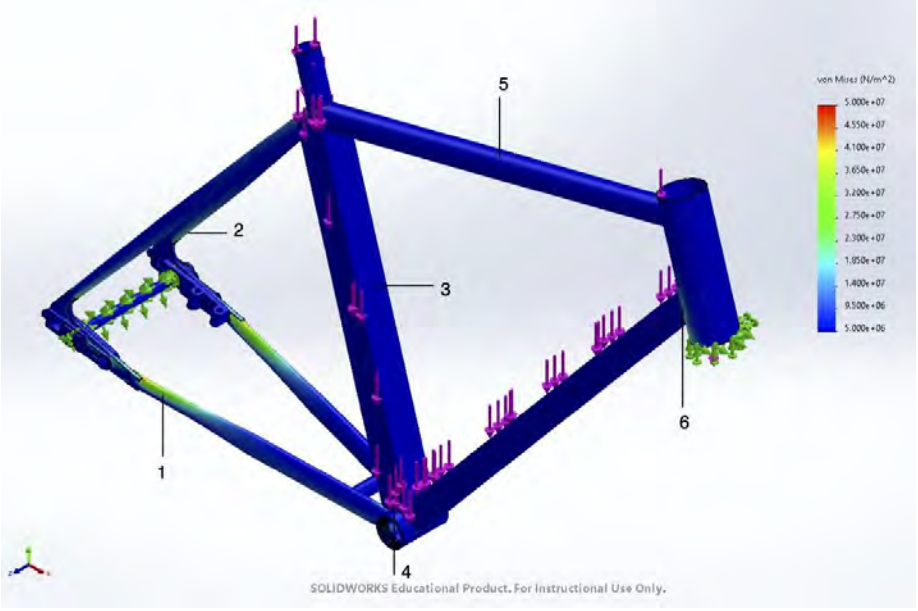

Figure 36: A von Mises stress plot of the frame showing areas of stress concentration.

The stresses in the chain stays are the highest due to the joining mechanism between its thin tubing and the dropouts. According to the FEA, these stresses exceed those experienced in the seat stays. Furthermore, the loading mechanics of the seat stays and chain stays are similar. Finally, the dimensions of the two components are similar as well. With this insight, only the chain stays will be tested. If they are able to survive testing, the seat stays are likely safe to use as well.

4.3.2 Testing Procedure and Performance Requirements

The new testing procedures were designed to replicate the British Standards as closely as possible, while minimising the number of additional components and testing rigs required. As a result, the frequency, number of cycles and forces have been kept the same. Additionally, all striker masses and impact forces were kept at similar values. These tests were designed to be a decomposed version of the full frame tests.

Test 1: Chain stay and Dropout Fatigue

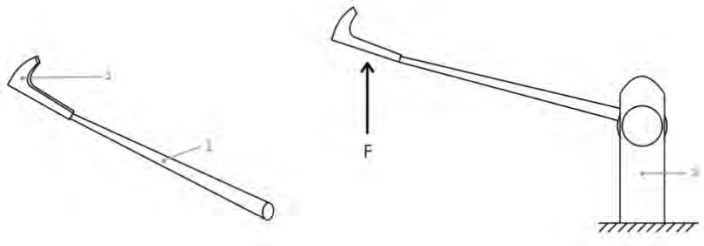

1	Chain stay
2	Drop out plate
3	Rigid Fixture

Figure 37: Diagram of chain stay and dropout fatigue test.

This sub assembly is expected to be under fatigue loading due to the shocks transferred through the rear wheel into the rear axle. As a result, upward cyclical forces can be expected. The expected failure point is the joint between the drop out and chain stay. The subassembly must be attached to a rigid fixture. The test rig requires a force F = 1100N at frequency 10Hz. In the rig, the force is applied for 100,000 cycles, where each cycle involves the application and removal of the force. During testing, there shall be no visible cracks or fractures in the assembly. Furthermore, there should be no separation of parts at the frame's joints. Finally, the peak-to-peak values of displacements at the point of force application shall not increase by more than 20% of the initial displacement values. For all fatigue tests, the initial value of displacement is measured after 1,000 cycles and before 2,000 cycles.

Test 2: Box Section Seat Tube Buckling

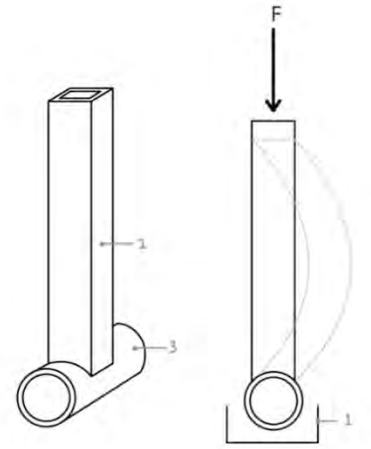

1	Instron Machine Clamp
2	Box Section Seat Tube
3	Bottom Bracket

Figure 38: Diagram of box section seat tube buckling test

Since the weight of the rider is centred directly above the seat tube, it is prone to buckling. Even though the FEA model does not predict high stresses in this tube, the assumption is that the rider is only 80kg in mass. Hence, engineering insight beyond the FEA models led to a decision to test seat tube buckling.

The set-up requires clamping the bottom bracket using an Instron fatigue machine. Following which, a force F must be applied and increased until visible buckling of the seat tube. Record this force and ensure that it is above 1000N in order to verify that it can take the weight of the rider without failure.

Test 3: Bottom Bracket Brazed Joint Fatigue

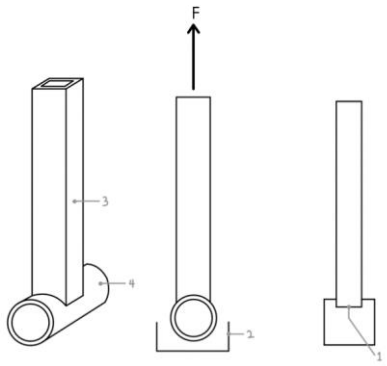

1	Brazed Joint
2	Instron Machine Clamp
3	Box Section Seat Tube
4	Bottom Bracket

Figure 39: Diagram of Bottom Bracket Brazed Joint Fatigue Test

This part of the frame is expected to be exposed to the most consistently cyclical force as a result of pedalling. As a result, it is important to test the ability of the brazed joint to withstand this fatigue. The set-up is similar to Test 2. However, this time the force must be applied upwards at the top end of the seat tube in order to simulate the tensile forces generated due to downward pedalling.

During the test, a force F = 1100N at frequency 10Hz must be applied. Apply this force for 100,000 cycles, where each cycle involves the application and removal of the force. During testing, there shall be no visible cracks or fractures in the assembly. Furthermore, there should be no separation of parts at the brazed joint. Finally, the peak-to-peak values of displacements at the point of force application shall not increase by more than 20% of the initial displacement values. For all fatigue tests, the initial value of displacement is measured after 1,000 cycles and before 2,000 cycles.

Test 4: Top Tube Impact Fracture

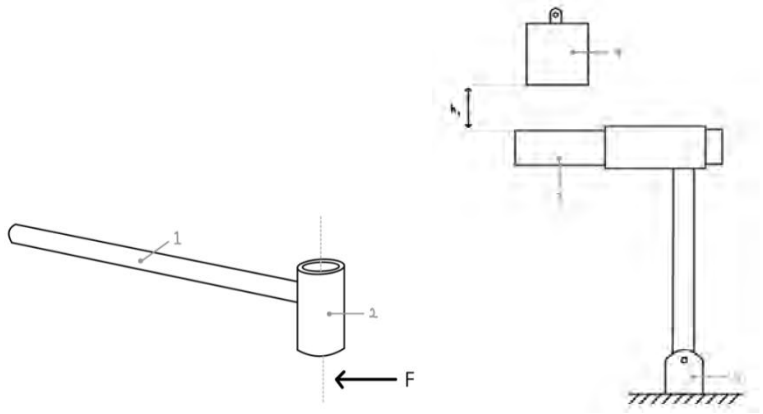

1	Top Tube
2	Head Tube
3	Circular Impact Bar
4	Striker Mass (22.5 kg)
5	Rigid Fixture

Figure 40: Diagram of Top Tube Impact Fracture Test

The frame must be strong enough to withstand sudden horizontal impact due to a head-on collision. The most likely component to deform or fracture under direct impact is the top tube. During a collision, the most likely point of contact is the front wheel, which will transfer the shock through the steering assembly into the head tube. As a result, a cantilever-like force mechanism is generated. This mechanism has been replicated in the test.

The test set up requires mounting the top tube against a rigid fixture. An impact bar must be inserted into the head tube, with a protruding length similar to the head tube. During the test, a striker mass of 22.5 kg must be dropped from a height h_1 = 360mm. There should be no visible fracture of the top tube.

Test 5: Down Tube Brazed Joint Pedalling Fatigue

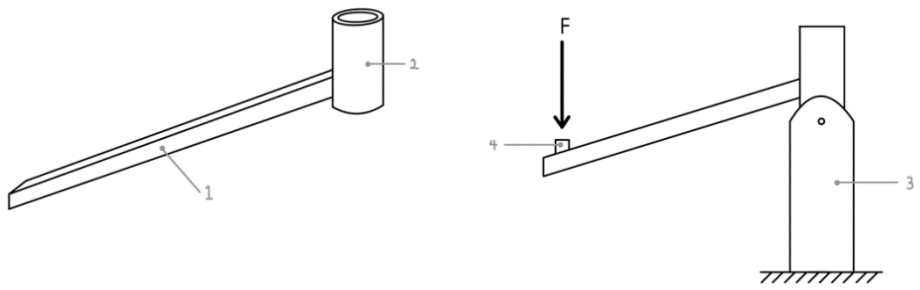

1	Down Tube
2	Head Tube
3	Rigid Fixture
4	Flat Knob

Figure 41: Diagram of Down Tube Brazed Joint Pedalling Fatigue Test

The down tube is likely to experience downward pedalling forces near the end attached to the bottom bracket. These forces are likely to cause deformations near the brazing joint between the head tube and the down tube, which likely contains higher stress concentrations. As this was a likely failure point, a fatigue test for the brazing joint was designed.

The test set up involves attaching the head tube to a rigid fixture. Then, a vertical force is applied at the far end of the down tube, simulating a cantilever. The force is applied against a flat knob for proper contact. During the test, a force F = 1100N at frequency 10Hz must be applied. Apply this force for 100,000 cycles, where each cycle involves the application and removal of the force. During testing, there shall be no visible cracks or fractures in the assembly. Furthermore, there should be no separation of parts at the brazed joint. Finally, the peak-to-peak values of displacements at the point of force application shall not increase by more than 20% of the initial displacement values.

4.3.3 Testing Resources Considerations

While designing the tests, it was also important to consider the availability of facilities and the resource intensiveness of each test. Table 12 shown below is a summary of the required resources and testing facilities.

Table 12: Required resources and testing facilities.

Test Name	Required Materials for Test Components	Required Facility/Machine	Test Duration
Test 1: Chain stay and Dropout Fatigue	• Stainless Steel (304 2B) • Omnicrom	Instron 8872 Servohydraulic Fatigue Testing System (Mechanical Engineering Department)	180 minutes
Test 2: Box Section Seat Tube Buckling	• Mild Steel E220 • Omnicrom	100T ESH HR (Mechanical Engineering Department)	30 minutes
Test 3: Bottom Bracket Brazed Joint Fatigue	• Mild Steel E220 • XCR Steel	Instron 8872 Servohydraulic Fatigue Testing System (Mechanical Engineering Department)	180 minutes
Test 4: Top Tube Impact Fracture	• Mild Steel E220 • Omnicrom	Impact Rig (Civil Engineering Department)	30 minutes
Test 5: Down Tube Brazed Joint Pedalling Fatigue	• Mild Steel E220	Instron 8872 Servohydraulic Fatigue Testing System (Mechanical Engineering Department)	180 minutes

5 Discussion

5.1 Assessment of design objectives.

As described in Section 4, the tests were altered from the British Standard descriptions. This was updated in the design specification as it became clear that these tests were not possible, but as discussed there was the question of conformity to government regulations, since this was proposed in the original brief and was interpreted by the group as indicating conformation to the British Standard regulations. This could be regarded as a missed target in the design, but it is one that would need a larger budget and production run to be obtainable. The stated design safety factor of 3 was not met in all cases. Although the dropouts and the rear thru axle exceeded this, the frame did not – owing to the presence of some stress concentration factors, and features present within the CAD, as is discussed later in this section.

Section 5.2 discusses the budget allocation of the team, and whilst the design was unable to be kept under the original budget, the other subgroups also encountered this issue. Hence, the initial aim of staying within the £1000 budget was not achieved in this iteration, but the reasons for this are discussed later.

The clearances for the subassemblies within the frame are very small in this iteration. This is in part due to the envelope, agreed early in the project, being exceeded by the battery group, and the shape of the motor group's assembly changing. The initial envelope specified for the motor group was 350 mm long by 40 mm tall by 55 mm wide. The final dimensions ended up being 350 mm by 80 mm by 55 mm. This caused very small gaps (~1, 3 mm) between the battery casing and the top tube at one end, and the battery casing and the motor mounting plate at the other. This had the effect of necessitating a redesign of the battery mounting mechanism, to allow the battery to fit in sideways. It was then decided that the battery would be bolted to the frame, which did in fact ensure that the integrated criteria of the initial brief was fulfilled. This caused the holes which have been drilled in the downtube to have very tight tolerances to ensure that the battery fits in, since the motor plate will be welded to the frame prior to the installation of the battery.

In the initial form in which it was considered, the testing was unsuitable for this project. This has led to changes being made to enable the group to test as faithfully as possible to the British Standard test procedures. This is discussed further in Section 5.2.

The original PDS generated by the frame team specified that testing would occur in line with these standards. The PDS has been updated to reflect the changes to testing, however, the initial brief stated that the bike itself was required to be government compliant. The group

interpreted this as conformity with this British standard, as on the UK Government website, for full classification as a normal bicycle, the bicycle must meet the ‘EAPC regulations’ (Electric bikes: licensing, tax and insurance, n.d.).

In the first version of the Quality Plan, and due to the brief set out at the start of the project, it was considered that the testing methods listed in the standard would be employed. However, as the project progressed, especially with the amendment from the department to remove the building of the second iteration, it was then decided that to test a frame in this manner, which would cause damage and possibly destruction of the frame, would leave not only the group without a product of their work up until the redesign, but would also remove from other groups the opportunity to mount their respective subassemblies on a frame, defeating the purpose of the integration nature of this project.

The constraints and conditions used within the FEA simulations are believed to be accurate to how the bike will be loaded during normal riding, regarding the weights on the frame and the ways in which the frame is free to move. The constraints represent being supported by the headset assembly and the rear axle when the bike is fully assembled, and the loads are calculated simply from the masses provided by the other subassemblies.

Regarding the final simulation, confidence is gained in the frame from the averages and the plots, since the low average values agree well with what is shown by the Solidworks simulation. As referenced in Section 3.5, the values obtained from the 2D MATLAB simulation also give weight to the average and RMS stresses being as low as they are. It can be seen from the plots that every component of the frame is, in the vast majority, shown to have very low stresses present. Even where stress concentration factors are present, they are in locations for which there are mitigating factors to be considered.

The minimum safety factor is significantly lower than previous simulations, and there are a few potential reasons for this. The change in constraint means the frame is now modelled with no completely constrained geometry, i.e., that the dropouts are free to rotate about the axis of the rear axle. This rotation may contribute to a change in the distribution and the concentration of the load around the dropouts and where they attach to the rear seat stay.

A minor simplification in the CAD model which could have significant impact on the overall simulated strength is the seat stay to dropout interface. The model features a flat cut on one end of the seat stay with a rectangular cut-out for the dropout to braze on to. This leaves a few exposed corners in the joint, likely to be stress raisers. For manufacturing, this interface will feature dual-purpose weld caps. Firstly, the caps provide two additional edges for brazing which increases the strength of the joint. Moreover, the caps follow the profile of the seat stays and

seal the open ends from the elements. Dropouts are attached this way on mass-production bikes, and the widespread use of this fastening method lends credence to the strength of joining the dropouts in such a manner.

Despite the stress concentrations shown in the final FEA model, and the relatively low minimum safety factor of the frame (compared to that specified in the PDS), there is further confidence in the frame's design as it uses widely employed materials in a configuration which is not dissimilar to bicycle frames which are manufactured and used daily around the world. Where stress concentrations do occur on the tubes in the frame, it is common that the peaks in stress are at or near the boundaries between tubes. Once more, this is to be expected as cuts have been made either to ensure the tube fits the component to which it connects, or to add a component in – the example being the dropouts. The joins created by brazing will reinforce the stress concentrations at the cuts on the tubing, since the braze will add filler material around the join.

5.2 Budget

Since the frame team is responsible for purchasing essential bike parts from various stores and workshops, a budget table was compiled with their respective specifications and reference links. Figure 35 shows an extract of the full table.

Parts to Buy	Size	Compatibility	Material	Brand	Stock Numb	Manufacturing Process	Manufacturer/Supplier	Estimated Cost (excl VAT)	Estimated Cost (incl VAT)	Reference Link
Seatpost	⌀27.2 mm, 350/400 mm Length		6061 (site spec)	Brand-x	N/A	N/A	Wiggle	£	15.00	https://www.wiggle.co.uk
Comfort Saddle			Foam, gel padding, steel alloy rails (site spec)	Brand-x	N/A	N/A	Wiggle	£	15.00	https://www.wiggle.co.uk
Seatpost Clamp	Inner ⌀ 27.2 mm, Outer ⌀ 28.6 mm		6000-series (site spec)	Brand-x	N/A	N/A	Wiggle	£	4.00	https://www.wiggle.co.uk
Wheelset (Half Cost, split with steering team)	700c, 142mm 12mm thru axle hub	disc brakes (center lock)	Aluminium Alloy (site spec)	Merlin	N/A	N/A	Merlin	£	69.50	Total cost = 139; split betv
Accessories Cost								**£**	**103.50**	
Top Tube	Outer ⌀31.7 (butted inside), L=560 mm		Omnicrom steel	Columbus	SLFL11560		The Bicycle Academy	Accounted for within Bike Academy quote		https://www.framebuildin
Seat Tube	Outer ⌀28.6 mm, nominal inner ⌀27.2 mm (butted inside), L=560 mm		Omnicrom steel	Columbus	SLFLI13560		The Bicycle Academy	Accounted for within Bike Academy quote		https://www.framebuildin
Seat Stays	Oval (16x30) mm (butted inside), L=410 mm		Omnicrom steel	Columbus	SLF7150V560		The Bicycle Academy	Accounted for within Bike Academy quote		https://www.framebuildin
ChainStays	Oval (19.5x25.5) mm (butted inside), L=420 mm		25CrMo4 Steel	Columbus	ZONI140V4ZO DX		The Bicycle Academy	Accounted for within Bike Academy quote		https://www.framebuildin
Bottom Bracket Shell	Outer ⌀40, L=68mm (english thread)		XCR	Columbus	ZSMJXCR		The Bicycle Academy	Accounted for within Bike Academy quote		https://www.framebuildin
Cutting							The Bicycle Academy	Accounted for within Bike Academy quote		
Jig Setup							The Bicycle Academy	Accounted for within Bike Academy quote		

Figure 42. An overview of the budget.

The initial given budget of this DMT project was £1000. Roughly £300 was planned to be spent on purchasing essential bike parts after market research regarding the price of these products. The rest, £700, would be spent on materials and manufacturing. However, the received quotes

from workshops were way beyond the budget limit and it became necessary to mitigate costs as much as possible.

Table 13: Summary version of full budget table.

	Example of Parts	Price (£)
Accessories	Seatpost, Saddle, Wheels	103.50
Bicycle Academy	Top Tube, Seat Tube	1075.00
Purchased Tubing	Thru Axle, Headtube	194.73
Manufacturing	Left and Right Dropouts	844.16
Fasteners	Socket Head Cap Screw	50.00
Painting	Power Coating	80.00
Shipment	N/A	51.03
Software	BikeCAD	30.20
Testing	Dummy Component Testing	750 (estimated)
Total Cost		3178.62

A summary version of the full budget table is shown above (Table 13). The total estimated cost of this DMT project would be £3178.62, and an extra funding request of £2500 before rough testing costs were computed. The larger-than-anticipated budget was caused by a few factors. Firstly, parts which could have been machined by the group (such as the thru axle) or CNC machined in the STW (the dropout plates) had to be outsourced, which increased their overall cost. Further to this, the one-off nature of the project also caused an increase in expenditure. Mitigation of this was attempted with the redesign of the dropout plates, some of the most if not the most expensive components, to be symmetrical. Even with this in place, the production run for all parts is still small (one or two of each part are being machined). Comparing to what would be borne per unit if the bike was to be sent for mass manufacture, this would add significant setup costs, especially in CNC processes. As shown in Figure 43, the least expensive option was chosen among multiple received quotes. In terms of accessories, bike parts other than wheels with specified requirements were all purchased from Wiggle, as it is the cheapest option in UK under the pandemic scheme. After discussing with other subgroups, the purchase of pedals was re-allocated to the gearbox team, and the cost of wheels would be evenly split with the steering group. This not only helped the frame team on budgeting, but also completed their respective final designs. Even though this is 3.2 times higher than the given budget, various approaches were considered and applied for cost mitigation, and the frame team believed that this is the optimal solution.

Turning	Protolabs	133.88	£	160.66	https://imperiallondon-my.sharepoint.com/	**STW:**		£250.00 excl material	Asked for 25 mm diam x 250 mm length 6061 Al	Matl cost: 4.41 excl VAT and delivery	Inclusive matl cost: 11.29	Total cost: 261.29
Turning, boring	Metals4U.co.uk	15.04	£	18.05	https://www.metals4u.co.uk/materials/stainless-steel/stainless-steel-tube/100393-p							
Extrusion; milling to desired length	Metals4U.co.uk	4.81	£	5.77	https://imperiallondon-my.sharepoint.com/							
Extrusion; milling to desired length	Metals4U.co.uk	8.54	£	10.25	https://imperiallondon-my.sharepoint.com/:i:/g/personal/tmh918_ic_ac_uk/EXvXMzZv6VVFgkfRhEwUWKUBIKQetjsB19wLglRkuVUpsA?e=EkBrvN							
			£	**194.73**		**Tridan:**			**Incl VAT:**		**MRT Castings**	**Incl VAT:**
CNC						£	1,370.00	£685 x2 - left and right dropout	£	1,644.00	£500 left & right dropouts	600.00
Laser Cut	LaserMaster	15.48	£	18.58	https://imperiallondon-my.sharepoint.com/							
Laser Cut	LaserMaster	9.52	£	11.42	https://imperiallondon-my.sharepoint.com/							
N/A	LaserMaster	150	£	180.00	https://imperiallondon-my.sharepoint.com/							
CNC	Protolabs	178.41	£	214.09	https://imperiallondon-my.sharepoint.com/	£	490.00		£	588.00		
CNC	Protolabs	133.92	£	160.70	https://imperiallondon-my.sharepoint.com/	£	465.00		£	558.00		
CNC	Protolabs	107.39	£	128.87	https://imperiallondon-my.sharepoint.com/	£	220.00		£	264.00		
CNC	Protolabs	108.75	£	130.50	https://imperiallondon-my.sharepoint.com/	£	225.00		£	270.00		
			£	**844.16**		£	2,770.00		£	3,324.00		
			£	**50.00**								
	Academy		**£**	**80.00**	**Liquid painting given as another option, £120; powder coating chosen to save costs and as intricate graphics not needed.**							

Figure 43. Comparison of different manufacturing methods

6 Conclusions

Overall, there is confidence that the bike will function as intended (under normal riding conditions) when manufactured. The components and manufacturing processes are believed to be sufficiently robust that the results of this first iteration will be operational. The bike does not meet the PDS specified safety factor of 3 everywhere, as demonstrated by FEA, but a redesign according to the results of the testing plan should rectify this, even if some components of the frame require alteration. As expected, stress concentrations will be mitigated and removed where possible, and the strength of the joins will be assessed so that this too can be modified if required. Such a process is anticipated, due to said low minimum safety factor. From this will come an increase in the overall integrity of the bike frame.

It would have been of great benefit to test to the British Standard specifications for this project, as this would clearly have highlighted areas for improvement in the frame, but the tests devised are regarded as being sufficient substitutes given the constraints faced by the team in terms of budget and facilities available, and being confined to a single-unit production run, rather than having a large batch of frames from which to destructively test.

The redesign will also allow the group to better accommodate subassemblies, with more clearly defined envelopes and less constrained overall packing as designs become more efficient using the test data.

7 References

Aalco. (2019) *Aluminium Alloy - Commercial Alloy - 6082 - T6~T651 Plate* Available from: https://www.aalco.co.uk/datasheets/Aluminium-Alloy_6082-T6~T651_148.ashx # [Accessed 26th February 2015]

Alcoa. (2012) *Understanding Extruded Aluminum Alloys.* Available from: *https://www.alcoa.com/alloymaterials/default.html* [Accessed 26th February 2015]

BSI. (2017) BS EN 15194:2017, *BSI Standards Publication.*

Carlton Reid. (2019) *When Will E-Bike Sales Overtake Sales Of Bicycles? For The Netherlands, That's Now*. Available from: https://www.forbes.com/sites/carltonreid/2019/03/02/when-will-e-bike-sales-overtake-sales-of-bicycles-for-the-netherlands-thats-now/?sh=49741f9c2e4a [Accessed 25th February 2015]

Claudia Wasko. (n.d.) *Why More States Need to Adopt the Three-Class eBike System* Available from: https://www.bosch-ebike.com/us/everything-about-the-ebike/stories/three-class-ebike-system/#:~:text=Class%201%3A%20eBikes%20that%20are,assisted%20speed%20of%2028%20mph. [Accessed 25th February 2021]

Claudia Wasko. (n.d.) *Hub-Drive vs. Mid-Drive eBikes: What to Know Before Buying* Available from: https://www.bosch-ebike.com/ca/everything-about-the-ebike/stories/hub-drive-vs-mid-drive-ebikes/#:~:text=For%20a%20mid-drive%20eBike,of%20riding%20a%20traditional%20bike. [Accessed 25th February 2021]

Columbus. (2020) *Steel Catalogue v1*. Available from: http://framebuilding.com/acrobat%20files/Columbus%202020%20Steel%20Catalogue%20v1%20web.pdf [Accessed 26th February 2015]

Covill, D., Begg, S., Elton, E., Milne, M., et al. (2014) Parametric Finite Element Analysis of Bicycle Frame Geometries. *Procedia Engineering*. 72441–446. Available from: doi:10.1016/j.proeng.2014.06.077.

Direct Voltage (n.d.) *Brushless Gear Hub Motor E-bike Motor For Electric Bicycle*. Available from: https://directvoltage.com/shop/ebikes/hub-motors/mxus-xf08-250w-brushless-gear-hub-motor-e-bike-motor/#content [Accessed 25th February 2021]

DMT Group 1-A. (2021). Design an E-bike frame: ME3 DMT Quality Plan Report. *Mechanical Engineering Department, Imperial College London*

Ebike portal. (n.d.) *Ogden Bolton Jr and His 1895 Hub Motor Ebike.* Available from: http://www.ebikeportal.com/history/ogden-bolton-jr-and-his-1895-hub-motor-ebike [Accessed 25th February 2021]

Engineers Academy. (2018) *Selecting Ideal Materials for Bicycle Frames Using Material Selection Charts.* Available from: https://www.youtube.com/watch?v=eRaxjdijGPg [Accessed 25th February 2021]

Engineering Materials-Tribology-Design. (2020) *Materials Selection for Mechanical Design. Ashby Map for Stiffness-based and Strength-based Design.* Available from: https://www.youtube.com/watch?v=iNVmoSDoufk [Accessed 25th February 2021]

Eric Hicks. (2012) *10 Point Hub Motor Break Down*. Available from: https://www.electricbike.com/hubmotors [Accessed 25th February 2021]

Evans Cycles. (n.d.) *Road Bike Sizing Guide*Available from: https://www.evanscycles.com/help/bike-sizing-road [Accessed 26th February 2015]

GOV.uk. (n.d.) *Electric bikes: licensing, tax and insurance.* Available from:

https://www.gov.uk/electric-bike-rules [Accessed 25th February 2021]

GREATEBIKE. (n.d.) *What type of motor is the best? What type of drive should I choose for my e-bike?* Available from: https://greatebike.eu/what-type-of-motor-is-best-for-my-e-bike#:~:text=Currently%2C%20we%20have%20two%20types,also%20called%20the%20mid%20drive [Accessed 25th February 2021]

GREATEBIKE. (n.d.) *What type of motor is the best? What type of drive should I choose for my e-bike?* Available from: https://greatebike.eu/what-type-of-motor-is-best-for-my-e-bike#:~:text=Currently%2C%20we%20have%20two%20types,also%20called%20the%20mid%20drive [Accessed 25th February 2021]

Halfords. (n.d.) *The E-Bike Forecast.* Available from: https://blog.halfords.com/the-ebike-forecast [Accessed 25th February 2021]

Holger Haubold. (2020) *The European e-bike market is booming, latest industry figures show – and there is potential for more.* Available from: https://ecf.com/news-and-events/news/european-e-bike-market-booming-latest-industry-figures-show-%E2%80%93-and-there#:~:text=In%202019%2C%20the%20sales%20of,compared%20to%20the%20year%20before. [Accessed 25th February 2021]

Jonathan Manning. (2016) *The Cyclist guide to frame stiffness.* Available from: https://www.cyclist.co.uk/in-depth/1310/the-cyclist-guide-to-frame-stiffness [Accessed 25th February 2021]

Lin, C.-C., Huang, S.-J. & Liu, C.-C. (2017) Structural analysis and optimization of bicycle frame designs. *Advances in Mechanical Engineering*. 9 (12), 168781401773951. Available from: doi:10.1177/1687814017739513.

Mecholic. (2015) Brazing - *Applications, Precautions, Advantages and Disadvantages.* Available from: https://www.mecholic.com/2015/12/applications-precautions-advantages-and-disadvantages-of-brazing [Accessed 25th February 2021]

Mikey G. (2019) *Batch E-Commuter: Finally, a $2,000 Bosch eBike.* Available from: https://electrek.co/2019/10/04/batch-ecommuter-review [Accessed 25th February 2021]

Nilesh Bothra. (2019) E-bikes are changing the way we move — *A glimpse into E-bike sales around the globe*. Available from: https://medium.com/calamus/e-bike-sales-worldwide-91c1df5da89a [Accessed 25th February 2021]

Paragon Machine Works. (n.d.) *Engineering drawings of sliding dropouts* Available from: https://paragonmachineworks.com/files/public-docs/DS0004R.PDF [Accessed 25th February 2021]

Paul Lee, Mark Casey & Craig Wigginton. (2020) *Cycling's technological transformation: Making bicycling faster, easier, and safer.* Available from: https://www2.deloitte.com/us/en/insights/industry/technology/technology-media-and-telecom-predictions/2020/bike-technology-transformation.html/#endnote-7 [Accessed 25th February 2021]

Pverdone. (2018) *Disc brake mounting systems* Available from: http://www.peterverdone.com/disc-brake-mounting-systems [Accessed 25th February 2021]

Science-engineering.co.uk. (n.d.) *What is Brazing? Process Advantage and Disadvantage.* Available from: https://www.science-engineering.co.uk/what-is-brazing-advantages-and-disadvantages/ [Accessed 25th February 2021]

Shimano Steps. (2019) *Examining attitudes towards e-bike usage in 11 European countries.* Available from: https://shimano-steps.com/e-bikes/europe/en/state-of-the-nation-report [Accessed 25th February 2021]

Specialized. (n.d.) *FIND YOUR BIKE SIZE & SADDLE HEIGHT.* Available from: https://www.specialized.com/gb/en/bike-sizing/app#/?mpl=184432 [Accessed 26th February 2015]

Ulrich Hansen. (2020). Finite Element Analysis and Applications Lecture Notes. *Mechanical Engineering Department, Imperial College London.*

Wu, ChiaChin. (2013). Static and dynamic analyses of mountain bikes and their riders. *University of Glasgow.*

.

8 Appendices

8.1 Initial hand calculation of forces along tubes

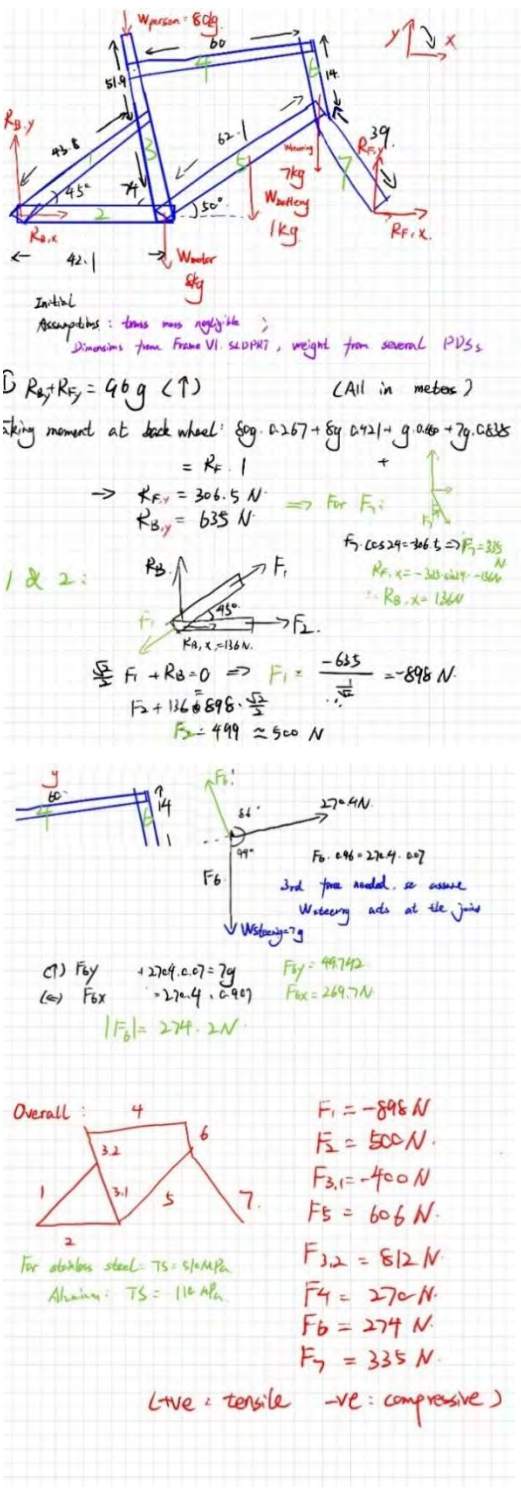

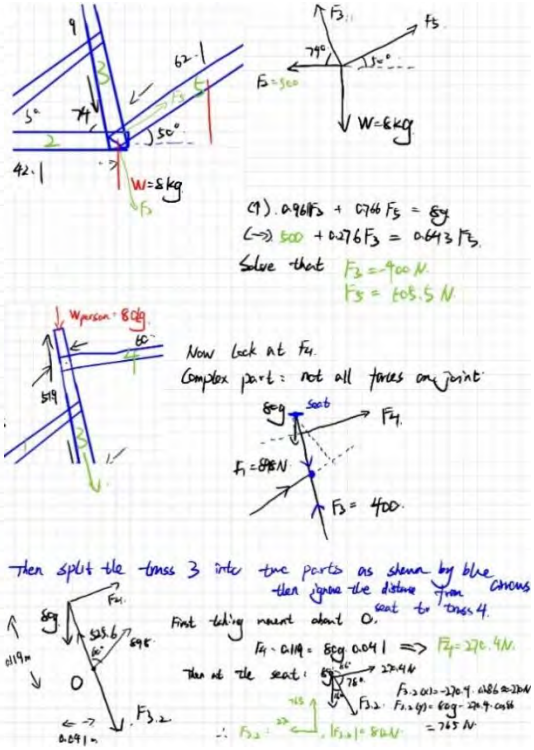

8.2 Example calculation for buckling check

For seattube, the force needed to buckle the tube P_L is:

$$P_L = \frac{\pi^2 EI}{L^2} = \frac{\pi^2 * 190 * 10^9 * 0.25\pi * (0.020^4 - 0.015^4)}{0.47223^2} = 722kN$$

Compare the actual load F with P_L

$$F = \sigma_{seattube} * A = 1.0051 * 10^7 * 57.9 * 10^{-6} = 0.589\text{kN}$$

This implies that the force the seat tube actually experiences is much lower than the force needed to buckle it, so for the seat tube buckling could be neglected.

8.3 MATLAB Code for FEA.

https://imperiallondon-my.sharepoint.com/:u:/g/personal/tmh918_ic_ac_uk/ESqZ63-VqslDtDw-o6HlCpEBpqKW-PamqQIA6KNCte89fw?e=lejVwo

8.4 Shimano Flat Mount Disc Brake Standard